Foxm1b transcription factor is essential for development of hepatocellular carcinomas and is negatively regulated by the p19^{ARF} tumor suppressor

Vladimir V. Kalinichenko,[1,2] Michael L. Major,[1,2] Xinhe Wang,[1] Vladimir Petrovic,[1] Joseph Kuechle,[1] Helena M. Yoder,[1] Margaret B. Dennewitz,[1] Brian Shin,[1] Abhishek Datta,[1] Pradip Raychaudhuri,[1] and Robert H. Costa[1,3]

[1]University of Illinois at Chicago, College of Medicine, Department of Biochemistry and Molecular Genetics, Chicago, Illinois 60607, USA

Hepatocellular carcinoma (HCC) is a leading cause of cancer-related deaths worldwide. Here, we provide evidence that the Forkhead Box (Fox) m1b (Foxm1b or Foxm1) transcription factor is essential for the development of HCC. Conditionally deleted *Foxm1b* mouse hepatocytes fail to proliferate and are highly resistant to developing HCC in response to a Diethylnitrosamine (DEN)/Phenobarbital (PB) liver tumor-induction protocol. The mechanism of resistance to HCC development is associated with nuclear accumulation of the cell cycle inhibitor p27^{Kip1} protein and reduced expression of the Cdk1-activator Cdc25B phosphatase. We showed that the Foxm1b transcription factor is a novel inhibitory target of the p19^{ARF} tumor suppressor. Furthermore, we demonstrated that conditional overexpression of Foxm1b protein in osteosarcoma U2OS cells greatly enhances anchorage-independent growth of cell colonies on soft agar. A p19^{ARF} 26–44 peptide containing nine D-Arg to enhance cellular uptake of the peptide was sufficient to significantly reduce both Foxm1b transcriptional activity and Foxm1b-induced growth of U2OS cell colonies on soft agar. These results suggest that this (D-Arg)$_9$-p19^{ARF} 26–44 peptide is a potential therapeutic inhibitor of Foxm1b function during cellular transformation. Our studies demonstrate that the Foxm1b transcription factor is required for proliferative expansion during tumor progression and constitutes a potential new target for therapy of human HCC tumors.

[*Keywords*: Forkhead Box; winged helix; liver cancer; p27Kip1; Cdc25B; Foxm1]

Received October 27, 2003; revised version accepted March 8, 2004.

Development of cancer is a multistep process requiring mutations in signaling pathways and cell cycle regulatory proteins that stimulate cellular proliferation and prevent apoptosis (Sherr and McCormick 2002). Cell division is tightly regulated at the G1/S (DNA replication) and G2/M (mitosis) transitions of the cell cycle by temporal activation of multiple cyclin-dependent kinases (Cdk) complexed with their corresponding cyclin regulatory subunits. In addition to assembly with a cyclin regulatory subunit, Cdk activity requires dephosphorylation of the Cdk catalytic subunit by the Cdc25A, Cdc25B, or Cdc25C protein phosphatase family, all of which are activated by the ras-mitogen activating protein kinase (MAPK) pathway (Sebastian et al. 1993; Trembley et al. 1996; Nilsson and Hoffmann 2000). The CIP/KIP family of Cdk inhibitor p21^{Cip1} and p27^{Kip1} proteins also negatively regulates Cdk activity (Sherr and Roberts 1999). It is well established that Cdk2 activity in complex with either Cyclin E or Cyclin A cooperates with Cyclin D-Cdk4/6 to phosphorylate the Retinoblastoma (RB) protein, which results in release of bound E2F transcription factor, allowing stimulation of genes required for S phase (Harbour and Dean 2000; Ishida et al. 2001). Moreover, stimulation of the Cdk1–Cyclin B complexes is required for M-phase progression by phosphorylating protein substrates essential for mitosis (Harbour and Dean 2000; Ishida et al. 2001).

Human hepatocellular carcinoma (HCC) is the fifth most common cancer, yet the third leading cause of cancer death worldwide, because late detection of this liver tumor renders current HCC therapy ineffective (Block et al. 2003; Varela et al. 2003). The primary etiology of human HCC involves hepatitis B virus (HBV) and HCV infections, resulting in chronic hepatic inflammatory in-

[2]**These two authors contributed equally to the work.**
[3]**Corresponding author.**
E-MAIL RobCosta@uic.edu; FAX (312) 355-4010.
Article and publication are at http://www.genesdev.org/cgi/doi/10.1101/gad.1200704.

jury and fibrosis (Block et al. 2003) as well as alcohol and nonviral-induced hepatic cirrhosis (Varela et al. 2003). In genetic mouse models of liver cancer, loss-of-function mutations in the p53 tumor-suppressor gene or gain-of-function mutations in either the Ras–MAPK, phosphoinositide 3-kinase (PI3K)-Akt or transforming growth factor α (TGFα)-signaling pathways are known to increase the incidence of HCC tumors (Sandgren et al. 1989, 1993; Wu et al. 1994; Thorgeirsson et al. 1998; Gomez-Angelats et al. 1999; Factor et al. 2001; Weihrauch et al. 2001). A well-established mouse liver tumor-induction protocol is available, and consists of a single postnatal injection of the tumor-initiator diethylnitrosamine (DEN), which induces hepatocyte DNA damage through DNA adduct formation. The initial DEN exposure is followed by continuous administration of the nongenotoxic liver tumor promoter phenobarbital (PB), which mediates hepatocyte hypertrophy (Tamano et al. 1994; Sargent et al. 1996; Kalinina et al. 2003).

The ARF/INK4A locus encodes two distinct tumor suppressors, the Cdk inhibitor $p16^{INK4A}$ and the 19-kD alternative reading frame (ARF) protein (14 kD ARF protein in humans) that are translated from different reading frames on exon 2 (Quelle et al. 1995; Sherr 1998). Increased levels of the $p19^{ARF}$ protein are induced in response to oncogenic transformation, and it mediates cell cycle arrest by increasing stability of the p53 tumor suppressor (Quelle et al. 1995; Kamijo et al. 1997). The $p19^{ARF}$ (p19) protein targets the p53 negative regulator Mdm2 to the nucleolus, thus stabilizing the p53 transcription factor, which regulates genes mediating G1 cell cycle arrest and/or apoptosis (Palmero et al. 1998; Pomerantz et al. 1998; Weber et al. 1999). The p19 protein also mediates p53-independent cell cycle arrest, because the p19 protein targets the E2F1 protein to the nucleolus, thus preventing E2F1 transcriptional activation of S-phase promoting target genes (Martelli et al. 2001; Datta et al. 2002). Loss of p19 function is a critical event for tumor promotion, as evidenced by extinguished expression of the p19 protein in a variety of tumors through DNA methylation and silencing of the p19 promoter region (Sherr and McCormick 2002). Furthermore, $p19^{ARF-/-}$ mice are susceptible to developing spontaneous tumors (Kamijo et al. 1997, 1999), underscoring the important role of the p19 tumor suppressor in preventing tumorigenesis.

The mammalian Forkhead Box (Fox) family of transcription factors consists of >50 mammalian proteins (Kaestner et al. 2000) that share homology in the winged helix DNA-binding domain (Clark et al. 1993). The Foxm1b protein (Foxm1, previously known as HFH-11, Trident, WIN, MPP2) protein is a proliferation-specific member of the Fox family of transcription factors (Korver et al. 1997; Yao et al. 1997; Ye et al. 1997). During liver regeneration, Foxm1b expression is markedly induced at the G1/S transition and continues throughout the period of hepatic cell proliferation (Ye et al. 1997). Use of the Transthyretin (TTR) promoter to prematurely express the Foxm1b (Hfh-11B) cDNA in regenerating liver of transgenic (TG) mice accelerated the onset of hepatocyte DNA replication and mitosis by stimulating earlier expression of cell cycle regulatory genes (Ye et al. 1999; Wang et al. 2001a; Costa et al. 2003). Furthermore, preventing the decline of hepatic expression of Foxm1b in 12-month-old (old-aged) TTR-Foxm1b TG mice is sufficient to increase regenerating hepatocyte proliferation to levels found in young regenerating liver (Wang et al. 2001b; Costa et al. 2003). In addition to re-establishing expression of cell cycle regulatory genes, levels of the Cdk inhibitor $p27^{kip1}$ protein were diminished when Foxm1b expression was restored in old-aged regenerating liver (Wang et al. 2002b; Krupczak-Hollis et al. 2003). More recent TG mouse studies demonstrate that ubiquitous expression of the Foxm1b transgene protein accelerated proliferation of distinct pulmonary cell types following lung injury, indicating that Foxm1b regulates proliferation of cells other than hepatocytes (Kalinichenko et al. 2003).

Using the Albumin enhancer and promoter-driven Cre recombinase transgene (Alb–Cre) to mediate hepatocyte-specific deletion of the *Foxm1b* fl/fl allele, we demonstrated that Foxm1b is essential for hepatocyte DNA replication and mitosis during liver regeneration (Wang et al. 2002a). Reduced hepatocyte proliferation was associated with increased nuclear protein levels of Cdk inhibitor $p21^{Cip1}$ and reduced protein expression of Cdc25B phosphatase, leading to decreased Cdk1 and Cdk2 activation required for cell cycle progression (Wang et al. 2002a). Furthermore, embryonic *Foxm1b* (*Trident*)$^{-/-}$ hepatocytes and cardiomyocytes exhibited an aberrant polyploid phenotype, suggesting that Foxm1b is required for coupling DNA replication with mitosis in these cell types during development (Korver et al. 1998). Analysis of microarrays with HCC samples demonstrated that expression of Foxm1b (Foxm1) was increased in HCC (Okabe et al. 2001). However, whether Foxm1b function is essential for development of HCC remained to be determined.

Here, we used a DEN/PB liver tumor-induction protocol to demonstrate that Alb–Cre *Foxm1b*$^{-/-}$ mouse hepatocytes fail to undergo proliferation and are highly resistant to developing HCC following DEN/PB liver tumor induction. The mechanism of resistance to HCC development in *Foxm1b*$^{-/-}$ hepatocytes involves sustained nuclear levels of the Cdk inhibitor $p27^{Kip1}$ protein and diminished expression of M-phase promoting Cdc25B phosphatase. We showed that hepatic expression of $p19^{ARF}$ tumor suppressor was transiently induced during DEN/PB tumor initiation and that the $p19^{ARF}$ 26–44 sequences were sufficient to associate with and inhibit Foxm1b transcriptional activity. Furthermore, we demonstrated that increased levels of Foxm1b protein in osteosarcoma U2OS cells stimulated anchorage-independent growth, as evidenced by increased number and size of cell colonies using a soft agar assay. Treatment of U2OS cells with a membrane transducing $(D\text{-}Arg)_9$ $p19^{ARF}$ 26–44 peptide significantly diminished Foxm1b-induced growth of U2OS cell colonies on soft agar, suggesting that this $p19^{ARF}$ peptide is an effective therapeutic inhibitor of Foxm1b function. These studies suggest

that Foxm1b is essential for development of HCC and required for the proliferative expansion of liver cancer.

Results

Alb–Cre Foxm1b$^{-/-}$ *livers fail to develop hepatic adenomas or hepatocellular carcinomas after DEN/PB treatment*

Hepatocyte-specific deletion of the *Foxm1b* fl/fl targeted allele with the Alb–Cre recombinase transgene demonstrated that *Foxm1b* is essential for mediating hepatocyte DNA replication and mitosis in regenerating mouse liver (Wang et al. 2002a). We therefore wanted to determine whether Foxm1b is required for proliferative expansion during mouse liver tumor formation using a well-established DEN/PB liver tumor-induction protocol (Tamano et al. 1994; Sargent et al. 1996; Kalinina et al. 2003). At 14 d postnatally, we gave the entire mouse litter containing both *Foxm1b* fl/fl (control) and Alb–Cre *Foxm1b*$^{-/-}$ (experimental) pups a single intraperitoneal injection of the tumor initiator DEN. Two weeks later, the mice were placed on drinking water containing 0.05% of the liver tumor promoter PB for the duration of the liver tumor-induction experiment. The Alb–Cre completely deletes the *Foxm1b* fl/fl allele in hepatocytes by 6 wk after birth (Postic and Magnuson 2000), and therefore, the *Foxm1b* allele is present during the DEN-mediated DNA damage (tumor initiation). Using this DEN/PB liver tumor-induction protocol, male mice are more susceptible to development of liver tumors exhibiting hepatocellular adenomas and HCC after 23 and 33 wk of DEN/PB exposure, respectively (Tamano et al. 1994; Sargent et al. 1996; Kalinina et al. 2003).

On the basis of these published studies, we examined for liver tumors in eight control *Foxm1b* fl/fl mice and 11 experimental Alb–Cre *Foxm1b*$^{-/-}$ mice at 23 wk of DEN/PB exposure and seven control *Foxm1b* fl/fl and 13 experimental Alb–Cre *Foxm1b*$^{-/-}$ mice at 33 wk following DEN/PB treatment (Table 1). We also harvested livers from male *Foxm1b* fl/fl and Alb–Cre *Foxm1b*$^{-/-}$ mice after 6 wk of DEN/PB exposure to provide an early time point during liver tumor promotion. Liver sections were histologically stained with hematoxylin and eosin (H&E), and hepatocyte DNA replication was determined by immunofluorescent detection of BrdU that had been administered in drinking water 4 d before sacrificing the mice (Ledda-Columbano et al. 2002). After 23 wk of DEN/PB treatment, H&E-stained liver sections from *Foxm1b* fl/fl male mice revealed numerous hepatic adenomas with abundant BrdU labeling (Fig. 1C,D,M; Table 1). Highly proliferative HCCs with abundant BrdU labeling were visible in liver sections from each of the male control *Foxm1b* fl/fl mice following 33 wk of DEN/PB exposure (Fig. 1E,I,J,M; Table 1). Furthermore, significant numbers of hyperproliferative adenomas were found in liver sections from female and male *Foxm1b* fl/fl mice after 33 wk of DEN/PB treatment (Table 1). No hepatic adenomas or HCC were detected in male or female Alb–Cre *Foxm1b*$^{-/-}$ mice at either 23 or 33 wk following DEN/PB exposure (Fig. 1A,E,G; Table 1). At 6, 23, and 33 wk following DEN/PB treatment, low levels of BrdU incorporation were found in *Foxm1b*-deficient hepatocytes (Fig. 1B,H), which was ~30% of BrdU-labeling levels of *Foxm1b* fl/fl hepatocytes in nontumor regions following DEN/PB exposure (Fig. 1N). Fetal hepatocytes express abundant levels of α-fetoprotein (AFP), then its hepatic expression is extinguished postnatally, but AFP expression is reactivated in HCC (Kunnath and Locker 1983; Chen et al. 1997). We detected AFP and BrdU-positive immunofluorescent cells in the *Foxm1b* fl/fl HCC liver tumors induced by DEN/PB exposure, which identified proliferating AFP-positive hepatocellular carcinoma cells (Fig. 1K,L). These studies suggest that Foxm1b is required for proliferative expansion during tumor development of hepatic adenomas and HCC.

The previous experiments demonstrated that male Alb–Cre *Foxm1b*$^{-/-}$ mice are resistant to developing HCC in response to 33 wk of DEN/PB exposure, a treatment sufficient to induce multiple HCC tumors in male *Foxm1b* fl/fl mice (Table 1). We next treated control *Foxm1b* fl/fl and experimental Alb–Cre *Foxm1b*$^{-/-}$ mice with DEN/PB for 50 wk to determine whether *Foxm1b*-deficient livers were resistant to a prolonged hepatic tumor-induction protocol. After 50 wk of DEN/PB exposure, all nine female Alb–Cre *Foxm1b*$^{-/-}$ mice were devoid of any liver tumors, whereas HCC tumors were found in all four control female livers with one additional control female mouse dying prematurely (Fig. 1F). Following 50 wk of DEN/PB exposure, no liver tumors were found in two of the four male Alb–Cre *Foxm1b*$^{-/-}$ mice, whereas one male mouse exhibited hepatic adeno-

Table 1. *Number of tumors per cm^2 liver tissue after 23 or 33 wk of DEN/PB treatment*

	Foxm1b fl/fl mice				Alb-Cre *Foxm1b* $^{-/-}$ mice			
DEN/PB and sex	[a]# Mice	[b]Adenomas	# Mice	Carcinomas	# Mice	Adenomas	# Mice	Carcinomas
23 wk Male	3	14.2 ± 5.2	3	0.5 ± 1.0	6	0	6	0
33 wk Male	3	11.2 ± 0.6	3	3.8 ± 0.9	7	0	7	0
23 wk Female	5	3.5 ± 1.7	5	0	5	0	5	0
33 wk Female	4	21.0 ± 6.9	4	0	6	0	6	0

[a](# Mice) Number of mice (male or female) analyzed for liver tumors after either 23 or 33 wk of Diethylnitrosamine (DEN)/Phenobarbital (PB) treatment.
[b]Number of liver tumors per cm^2 liver tissue ±S.D. (adenomas or hepatocellular carcinomas greater than 0.1 mm in size) determined from Hematoxylin and Eosin-stained liver sections obtained from four different mouse liver lobes.

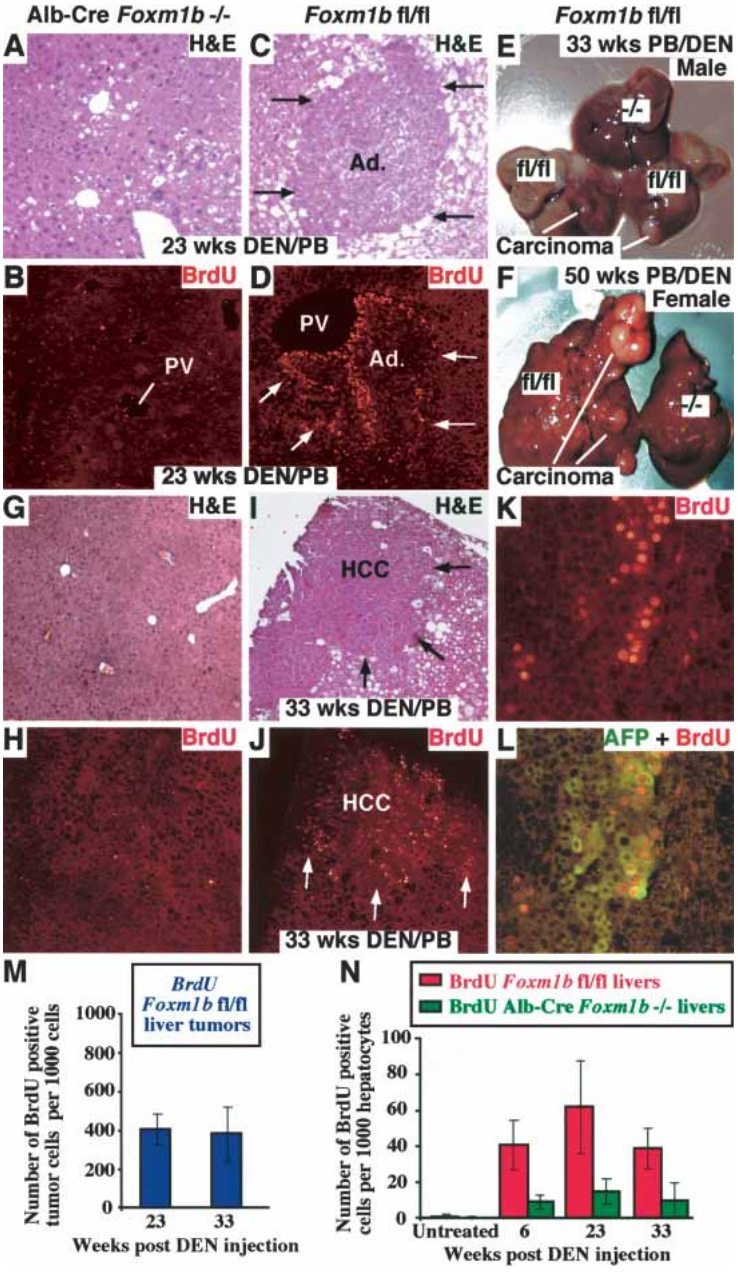

Figure 1. Alb–Cre *Foxm1b*$^{-/-}$ male mouse livers fail to develop adenomas at either 23 or 33 wk of DEN/PB exposure. Both *Foxm1b* fl/fl (control) and Alb–Cre *Foxm1b*$^{-/-}$ (experimental) mice were subjected to either 6, 23, or 33 wk of Diethylnitrosamine (DEN)/Phenobarbital (PB) exposure (Tamano et al. 1994; Sargent et al. 1996; Kalinina et al. 2003) and livers were dissected, paraformaldehyde fixed, paraffin embedded, and microtome sections were prepared. Liver sections were histologically stained with Hematoxylin and Eosin (H&E) and hepatocyte DNA replication was determined by immunofluorescent detection of BrdU incorporation. (*A–J*) Alb–Cre *Foxm1b*$^{-/-}$ male mice are resistant to developing adenomas or hepatocellular carcinomas (HCC) after either 23 or 33 wk of DEN/PB treatment. Arrows indicate margins of adenomas (*C*,*D*) or HCC (*I*,*J*) in either H&E- or BrdU-stained *Foxm1b* fl/fl livers after 23 or 33 wk of DEN/PB treatment. (*E*,*F*) Photograph of *Foxm1b* fl/fl mouse livers depicting HCC tumors after either 33 wk (*E*, male) or 50 wk (*F*, female) of DEN/PB exposure, whereas Alb–Cre *Foxm1b*$^{-/-}$ mice are resistant to liver tumor induction. (*K*,*L*) Same microscope field shows α-fetoprotein (AFP) and BrdU-positive immunofluorescent cells in the *Foxm1b* fl/fl HCC liver tumors, which identified proliferating AFP-positive HCC cells. (*M*) Graph of mean number of BrdU-positive tumor cells per 1000 cells (±S.D.) in the male *Foxm1b* fl/fl liver tumors induced by 23 or 33 wk of DEN/PB exposure. (*N*) Graph of mean number of BrdU-positive cells per 1000 hepatocytes (±S.D.) in nontumor regions of livers from male *Foxm1b* fl/fl or Alb–Cre *Foxm1b*$^{-/-}$ mice either untreated or after 6, 23, or 33 wk of DEN/PB exposure. We calculated the mean number (±S.D.) of BrdU-positive hepatocyte nuclei per 1000 cells or 200× field by counting the number of BrdU-positive hepatocyte nuclei using five different liver sections from three distinct male mice at the indicated times of DEN/PB exposure. Magnification: *A–D*, 100×; *G–J*, 50×, *K*,*L*, 400×.

mas, and the last male mouse displayed HCC tumors that were negative for Foxm1b protein staining (data not shown). These studies indicated that following prolonged DEN/PB tumor promotion, hepatic tumors were found in a subset of the male Alb–Cre *Foxm1b*$^{-/-}$ livers, suggesting that they develop secondary mutations that allowed tumor formation, bypassing the block in *Foxm1b*$^{-/-}$ hepatocyte proliferation.

Alb–Cre Foxm1b$^{-/-}$ *male mouse hepatocytes exhibited increased hypertrophy, but no increase in apoptosis in response to DEN/PB treatment*

To examine whether increased apoptosis contributed to the failure of male Alb–Cre *Foxm1b*$^{-/-}$ mice to develop liver tumors in response to 33 wk of DEN/PB treatment, we carried out TUNEL staining of liver sections from DEN/PB-treated mice. We found no statistically significant difference in hepatocyte apoptosis between Alb–Cre *Foxm1b*$^{-/-}$ and *Foxm1b* fl/fl mice after either 6, 23, or 33 wk of DEN/PB exposure (Fig. 2A–C). These results suggested that the absence of liver tumors in Alb–Cre *Foxm1b*$^{-/-}$ mice following DEN/PB exposure was not due to an increase in hepatocyte apoptosis.

Postmitotic adult mouse hepatocytes normally become tetraploid (4N) and octaploid (8N) with sporadic binuclear-containing hepatocytes (Steele et al. 1981). Prolonged treatment with the tumor promoter PB is known to further increase hepatocyte hypertrophy and ploidy (Sanders and Thorgeirsson 1999). Hypertrophy of

the Alb–Cre *Foxm1b*$^{-/-}$ hepatocytes was significantly increased compared with that of control hepatocytes (nontumor liver regions) at 23 wk of DEN/PB exposure (Fig. 2D,E). A centromere-specific FISH probe was used to show that Alb–Cre *Foxm1b*$^{-/-}$ hepatocyte nuclei possessed an increase in hybridizing chromosomes compared with control hepatocyte nuclei at 23 wk of DEN/PB treatment (Fig. 2F,G). To quantitate this increase in size, we counted the number of DAPI-stained hepatocyte nuclei (per 200× field) in *Foxm1b* fl/fl and Alb–Cre *Foxm1b*$^{-/-}$ liver sections and plotted these data for each of the time points following DEN/PB exposure (Fig. 2H). No statistically significant difference in hepatocyte hypertrophy was found in livers of *Foxm1b* fl/fl and Alb–Cre *Foxm1b*$^{-/-}$ mice that were either untreated or treated with DEN/PB for 6 wk (Fig. 2H). However, approximately half the number of hepatocyte nuclei per 200× field was found in Alb–Cre *Foxm1b*$^{-/-}$ livers compared with *Foxm1b* fl/fl control liver after either 23 or 33 wk of DEN/PB exposure (Fig. 2H). These data suggested that *Foxm1b*-deficient hepatocytes undergo greater hypertrophy and become more polyploid than *Foxm1b* fl/fl control hepatocytes at 23 and 33 wk of DEN/PB treatment. These results suggest that Alb–Cre *Foxm1b*$^{-/-}$ hepatocytes exhibited low levels of DNA replication (Fig. 1N) with a significant reduction in mitosis as was previously found in *Foxm1b*-deficient hepatocytes during liver regeneration and development (Korver et al. 1998; Wang et al. 2002a). Moreover, Alb–Cre *Foxm1b*$^{-/-}$ hepatocytes displayed normal serum levels of albumin, bilirubin, and glucose after 33 wk of DEN/PB exposure, indicating that their livers functioned normally (data not shown).

Hepatocyte expression of nuclear Foxm1b protein increases prior to liver tumor formation and continues during liver tumor progression

Immunohistochemical staining of liver sections with an antibody specific to Foxm1b protein demonstrated that untreated hepatocyte nuclei displayed no significant expression of the Foxm1b protein (Fig. 3A,B). Abundant nuclear staining of Foxm1b protein was detected in periportal *Foxm1b* fl/fl hepatocytes as early as 6 wk of DEN/PB (Fig. 3C), yet these hepatocytes failed to exhibit abun-

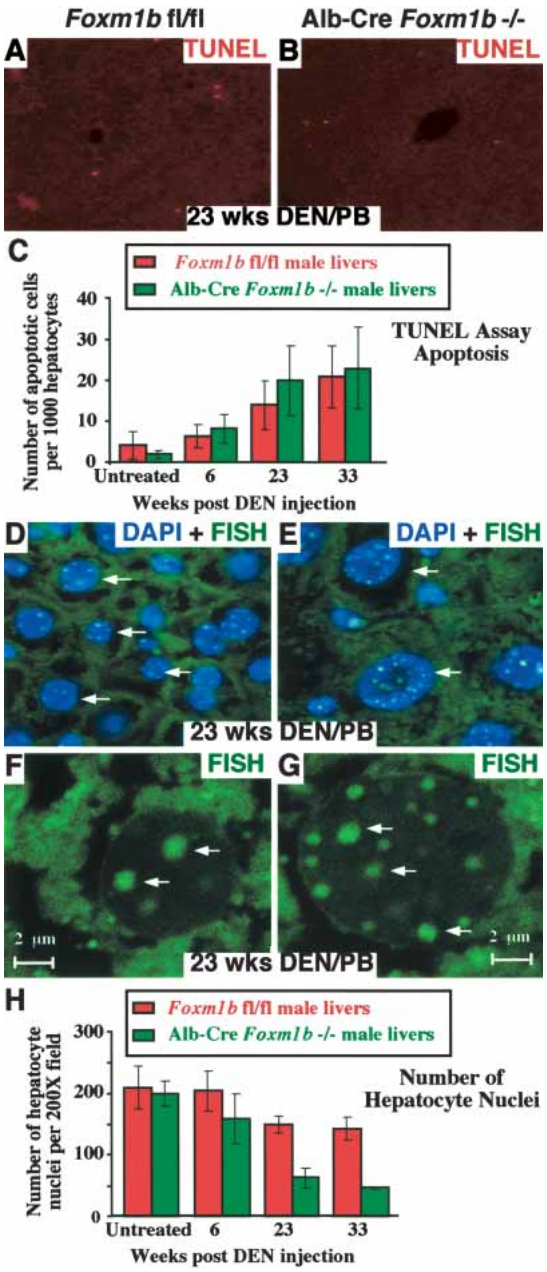

Figure 2. Alb–Cre *Foxm1b*$^{-/-}$ mouse hepatocytes exhibit no elevation in apoptosis and increased hypertrophy in response to DEN/PB treatments. (*A–C*) Alb–Cre *Foxm1b*$^{-/-}$ and *Foxm1b* fl/fl hepatocytes exhibited no differences in apoptosis levels following DEN/PB treatment. Florescent micrograph of TUNEL assay (*A*,*B*; 100×) demonstrated similar apoptosis levels in Alb–Cre *Foxm1b*$^{-/-}$ and *Foxm1b* fl/fl control after 23 wk of DEN/PB exposure. (*C*) Graph of number of apoptotic cells (TUNEL positive) per 1000 hepatocytes (±S.D.) in nontumor regions of livers from male *Foxm1b* fl/fl or Alb–Cre *Foxm1b*$^{-/-}$ mice after either 6, 23, or 33 wk of DEN/PB exposure or untreated. (*D–H*) Foxm1b-deficient hepatocytes became more polyploid than control hepatocytes after 23 wk of DEN/PB exposure. A centromere-specific mouse FISH probe was used to show that Alb–Cre *Foxm1b*$^{-/-}$ hepatocyte nuclei possessed an increase in the number of hybridizing chromosomes compared with control hepatocyte nuclei at 23 wk of DEN/PB treatment. Shown is a high-power magnification of hepatocytes, in which the nuclei were counterstained with DAPI (630×; *D*,*E*) or visualized by Laser Confocal microscopy (*F*,*G*; bar, 2 μm). (*H*) Graph of mean number of DAPI-stained hepatocyte nuclei per 200× field (±S.D.) in nontumor regions of livers from male *Foxm1b* fl/fl or Alb–Cre *Foxm1b*$^{-/-}$ mice either untreated or after 6, 23, or 33 wk of DEN/PB exposure. Diminished number of hepatocyte nuclei per field indicates increased hepatocyte hypertrophy. We calculated the mean number (±S.D.) of TUNEL or DAPI-positive hepatocyte nuclei per 1000 cells or 200× field by counting the number of positive hepatocyte nuclei using five different liver sections from three distinct male mice at the indicated times of DEN/PB exposure.

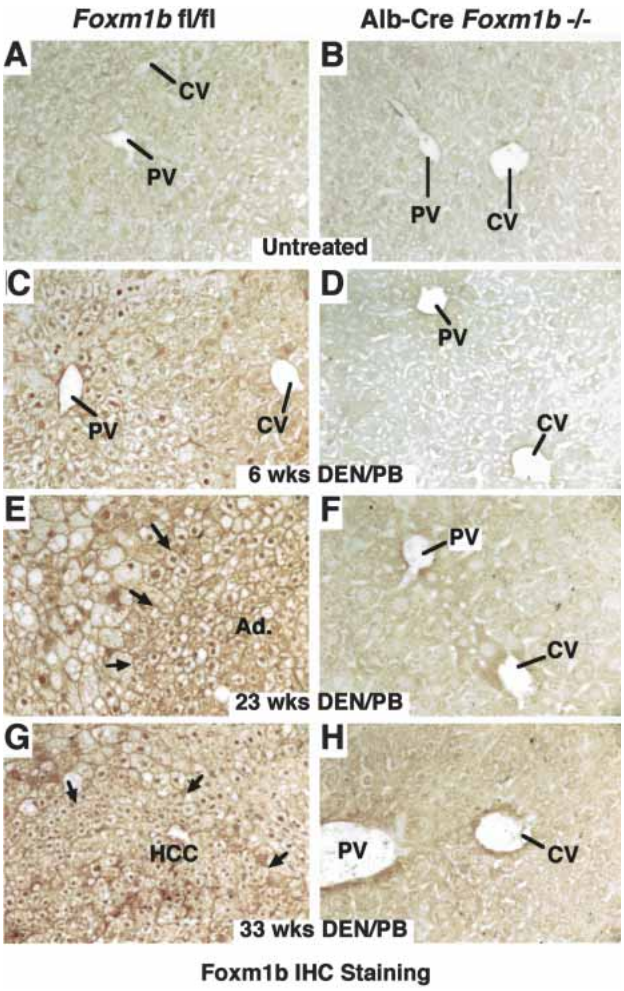

Figure 3. Hepatocyte nuclear expression of Foxm1b protein after DEN/PB liver tumor-induction protocol. Liver sections from *Foxm1b* fl/fl and Alb–Cre *Foxm1b*$^{-/-}$ mice either untreated or treated with DEN/PB for either 6, 23, or 33 wk were immunohistochemically stained for nuclear expression of Foxm1b protein. Abundant nuclear staining of Foxm1b protein is induced as early as 6 wk after DEN/PB exposure in *Foxm1b* fl/fl hepatocytes surrounding the portal vein (PV, *C*), but not in hepatocytes near the central vein (CV). (*C*,*E*,*G*) High levels of nuclear Foxm1b protein persisted in hyperproliferative hepatic adenomas and HCC (margins of tumor indicated by arrows). (*B*,*D*,*F*,*H*) As expected, nuclear staining of Foxm1b protein was not found in Alb–Cre *Foxm1b*$^{-/-}$ hepatocytes at any of the time points following DEN/PB treatment or in untreated liver (*A*,*B*). (PV) Portal vein; (CV) central vein. Magnification, 200×.

dant BrdU incorporation levels (Fig. 1N). High levels of nuclear Foxm1b protein persisted in hyperproliferative liver adenomas and HCC at 23 and 33 wk following DEN/PB exposure (Fig. 3E,G). As expected, nuclear staining of Foxm1b protein was not found in Alb–Cre *Foxm1b*$^{-/-}$ hepatocytes at any of the time points following DEN/PB treatment (Fig. 3D,F,H), confirming that the Alb–Cre transgene protein efficiently deletes the Foxm1b floxed-targeted allele in hepatocytes (Wang et al. 2002a). These studies demonstrate that hepatocyte nuclear levels of Foxm1b are induced in control hepatocytes prior to tumor formation following DEN/PB treatment, and that this nuclear expression persisted in hepatic adenomas and HCC.

Alb–Cre Foxm1b$^{-/-}$ *livers exhibit normal expression of GST-pi and CAR following DEN/PB treatment*

Our liver tumor studies demonstrated that loss of *Foxm1b* function blocks the proliferative expansion required for liver tumor growth (Fig. 1). We sought to examine whether the DEN/PB treatment of Alb–Cre *Foxm1b*$^{-/-}$ mice was able to induce hepatocyte expression of Glutathionine-S-transferase placental isoform (GST-pi), which is an early marker for altered enzyme foci in response to DEN/PB exposure (Hatayama et al. 1993). Altough GST-pi expression was not detected in liver sections of untreated control mice (Fig. 4A,B), both Alb–Cre *Foxm1b*$^{-/-}$ and *Foxm1b* fl/fl hepatocytes were strongly immunostained for GST-pi after 23 wk of DEN/PB treatment (Fig. 4C–F). Western blot analysis demonstrated that hepatic expression of GST-pi protein was induced as early as 6 wk following DEN/PB treatment in both Alb–Cre *Foxm1b*$^{-/-}$ and *Foxm1b* fl/fl livers with continued expression after 23 wk of DEN/PB exposure (Fig. 4G). PB stimulates nuclear translocation of the constitutive androstane receptor (CAR; Chawla et al. 2001). No difference in nuclear staining of the CAR receptor was found between *Foxm1b* fl/fl and Alb–Cre *Foxm1b*$^{-/-}$ hepatocytes following DEN/PB treatment (Fig. 4H,I), indicating that the *Foxm1b*-deficient hepatocytes are still responsive to the PB tumor promoter. Taken together, our data suggest that Alb–Cre *Foxm1b*$^{-/-}$ livers responded normally to DEN/PB tumor induction and expressed the altered enzyme foci GST-pi marker, but failed to undergo the proliferation required for tumor progression.

Persistent nuclear accumulation of the Cdk inhibitor p27^{Kip1} *protein and diminished Cdc25B expression in Alb–Cre* Foxm1b$^{-/-}$ *livers follows DEN/PB exposure*

Published liver regeneration studies with old-aged mice demonstrated that increased expression of Foxm1b protein restored hepatocyte proliferation to levels found in young regenerating liver and was associated with reduced hepatocyte nuclear expression of the Cdk inhibitor p27^{Kip1} protein (Wang et al. 2002b; Krupczak-Hollis et al. 2003). Consistent with these findings, persistent nuclear accumulation of hepatocyte p27^{Kip1} protein was found only in Alb–Cre *Foxm1b*$^{-/-}$ liver sections at 36 h after partial hepatectomy (PHx), indicating that loss of Foxm1b function was associated with nuclear accumulation of p27^{Kip1} protein in regenerating hepatocytes (Fig. 5A,B). Interestingly, these regenerating Alb–Cre *Foxm1b*$^{-/-}$ hepatocytes exhibited approximately half the BrdU incorporation rate of control *Foxm1b* fl/fl hepatocytes at 36 h post PHx, suggesting that reduced levels of hepatocyte DNA replication occurred in the presence of nuclear p27^{Kip1} protein (Wang et al. 2002a).

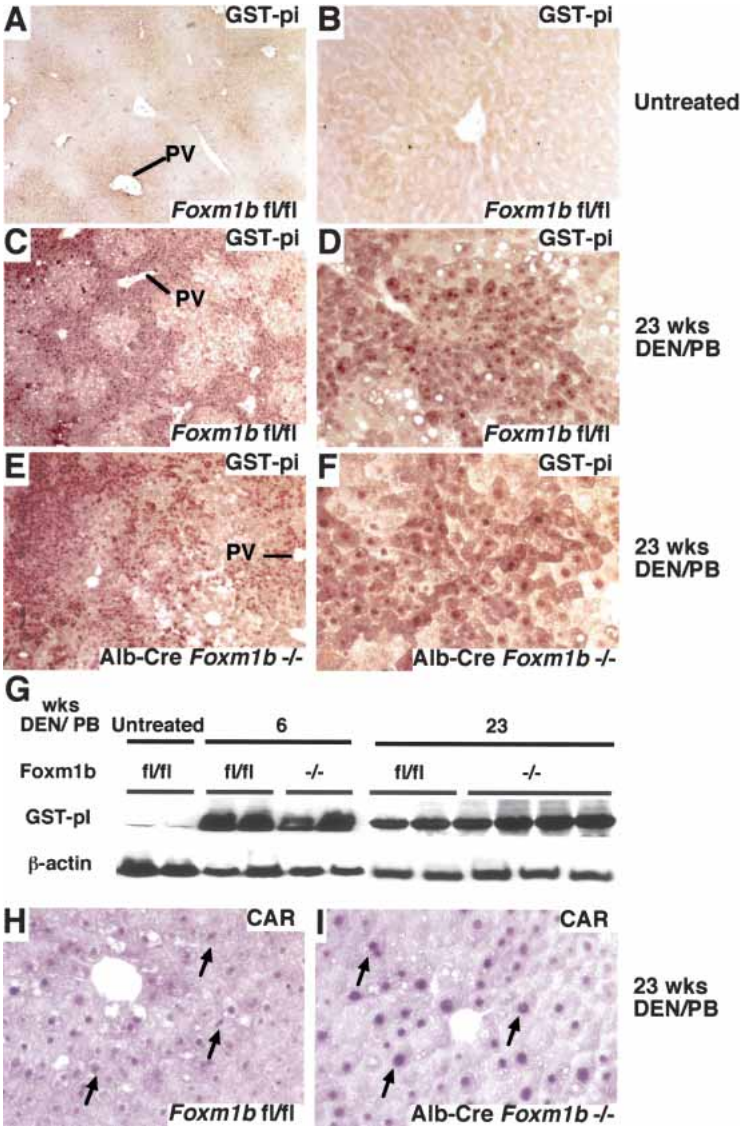

Figure 4. Alb–Cre *Foxm1b*$^{-/-}$ livers exhibit normal expression of GST-pi and CAR following DEN/PB treatment. Alb–Cre *Foxm1b*$^{-/-}$ and *Foxm1b* fl/fl livers isolated from male mice after 23 wk of DEN/PB exposure were immunohistochemically stained with antibody specific to GST-pi, which is an early marker for altered enzyme foci in response to DEN tumor initiation (Hatayama et al. 1993). Both Alb–Cre *Foxm1b*$^{-/-}$ and *Foxm1b* fl/fl hepatocytes were strongly immunostained for GST-pi after 23 wk of DEN/PB treatment (*C–F*), but its expression was not detected in untreated control *Foxm1b* fl/fl mouse liver (*A*,*B*). (*G*) Western blot analysis with liver protein extracts demonstrates that hepatic expression of GST-pi protein was induced as early as 6 wk following DEN/PB treatment, and that its hepatic expression continued following 23 wk of DEN/PB exposure. (*H*,*I*) Normal hepatocyte nuclear levels of the CAR nuclear receptor were found in male Alb–Cre *Foxm1b*$^{-/-}$ mice following DEN/PB treatment. Magnification: *A*,*C*,*E*, 50×; *B*,*D*,*F*,*H*,*I*, 200×.

We therefore examined for nuclear expression of p27^{Kip1} protein in mouse liver sections from untreated and DEN/PB-treated mice using immunohistochemical staining. Similar hepatocyte levels of nuclear p27^{Kip1} protein were found in untreated Alb–Cre *Foxm1b*$^{-/-}$ and *Foxm1b* fl/fl mice (Fig. 5C,D), a finding consistent with abundant nuclear expression of the Cdk inhibitor p27^{Kip1} protein in quiescent hepatocytes (Kwon et al. 2002). Hepatocyte nuclear staining of p27^{Kip1} protein was significantly diminished in *Foxm1b* fl/fl hepatocytes beginning at 6 wk and continuing through 33 wk after DEN/PB treatment (Fig. 5E,G,I,M). Furthermore, nuclear expression of p27^{Kip1} protein was undetectable in hepatic tumor cells at all time points following DEN/PB treatment (Fig. 5G,I). In contrast, hepatocyte nuclear staining of p27^{Kip1} protein was sustained in Alb–Cre *Foxm1b*$^{-/-}$ mice at 6, 23, and 33 wk after DEN/PB exposure (Fig. 5F,H,J,M). After 50 wk of DEN/PB treatment, nuclear staining of p27^{Kip1} protein was sustained in Female Alb–Cre *Foxm1b*$^{-/-}$ mouse hepatocytes (Fig. 5K,N), and these livers were resistant to development of adenomas and HCC. In contrast, male Alb–Cre *Foxm1b*$^{-/-}$ mouse hepatocytes exhibited nearly undetectable nuclear staining of p27^{Kip1} protein after 50 wk of DEN/PB exposure (Fig. 5L,N), and this was associated with 50% of the male Alb–Cre *Foxm1b*$^{-/-}$ mice developing liver tumors. These results suggest that an increase in liver tumor incidence in male mice, following prolonged response to DEN/PB treatment, was associated with loss of hepatocyte nuclear levels of p27^{Kip1} protein.

Surprisingly, Western blot analysis revealed similar levels of total p27^{Kip1} protein in *Foxm1b* fl/fl and Alb–Cre *Foxm1b*$^{-/-}$ liver extracts at 6, 23, or 33 wk following DEN/PB exposure (Fig. 6A). These results suggest that *Foxm1b* deficiency resulted in sustained hepatocyte levels of nuclear p27^{Kip1} protein after DEN/PB treatment without changing total expression of the p27^{Kip1} protein. We next stripped this Western blot and probed it sequen-

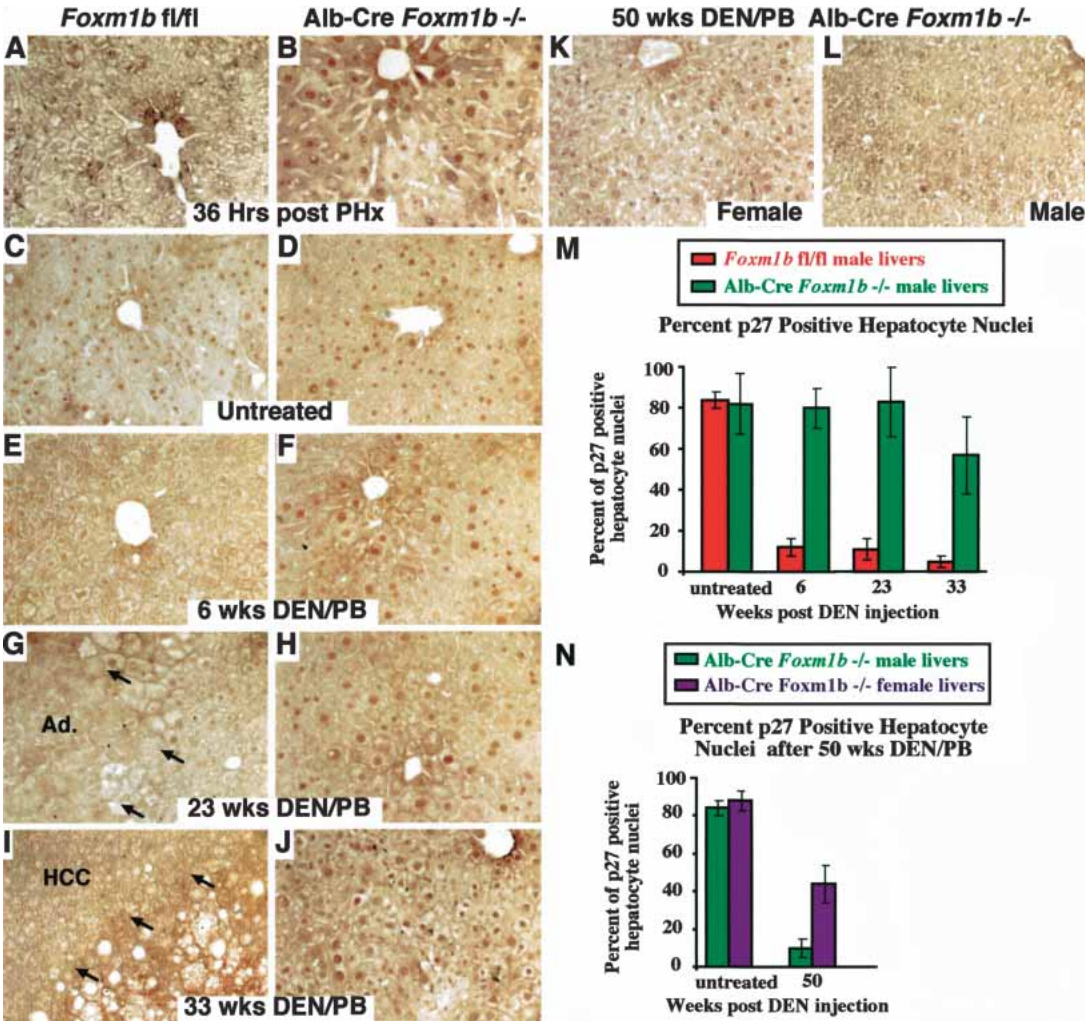

Figure 5. Alb–Cre *Foxm1b*$^{-/-}$ hepatocytes exhibit persistent increase in nuclear protein levels of Cdk inhibitor p27^{Kip1} following DEN/PB exposure. (*A*,*B*) Persistent nuclear accumulation of p27^{Kip1} protein was found only in Alb–Cre *Foxm1b*$^{-/-}$ liver sections at 36 h after partial hepatectomy (PHx), which still exhibited detectable BrdU incorporation (Wang et al. 2002a). (*C–J*) Liver sections from Alb–Cre *Foxm1b*$^{-/-}$ and *Foxm1b* fl/fl male mice after either untreated or after 6, 23, or 33 wk of DEN/PB exposure were used for immunohistochemical staining to examine for hepatocyte nuclear expression of p27^{Kip1} protein. (*I*,*J*) Liver sections from Alb–Cre *Foxm1b*$^{-/-}$ male and female mice after 50 wk of DEN/PB exposure were immunostained for nuclear levels of p27^{Kip1} protein. (*C*,*D*) No difference in hepatocyte nuclear staining of p27^{Kip1} protein was found in liver sections from untreated Alb–Cre *Foxm1b*$^{-/-}$ and *Foxm1b* fl/fl mice. (*C–J*) Hepatocyte nuclear staining of p27^{Kip1} protein was sustained only in male Alb–Cre *Foxm1b*$^{-/-}$ hepatocytes after 6, 23, or 33 wk of DEN/PB exposure (*E–J*) or female Alb–Cre *Foxm1b*$^{-/-}$ hepatocytes after 50 wk of DEN/PB treatment (*K*,*L*). (*E*,*G*) Margins of hepatic adenoma (Ad) or hepatocellular Carcinoma (HCC) are indicated by arrows. (*M*,*N*) Graph of percent p27^{Kip1}-positive hepatocyte nuclei per 200× field liver section during tumor progression. Number of hepatocyte nuclei per 200× section was determined by DAPI staining in adjacent sections. We calculated the mean ± S.D. percent of p27^{Kip1}-positive hepatocyte nuclei per 200× fields by counting hepatocyte nuclei positive for p27^{Kip1} staining using five different liver sections from three distinct male or female mice that were either untreated or after 6, 23, 33, or 50 wk of DEN/PB exposure. Magnification: *A–J*, 200×.

tially with antibodies specific to the Cdk1-activating Cdc25B or Cdc25C phosphatases. Published liver regeneration studies demonstrated that Foxm1b is essential for regulating transcription of the M-phase-promoting Cdc25B gene, but not the Cdc25C gene (Wang et al. 2002a). Consistent with these findings, *Foxm1b* fl/fl control livers exhibited a transient increase in expression of the M-phase-promoting Cdc25B phosphatase protein at 6 wk after DEN/PB exposure, whereas hepatic levels of Cdc25B protein were significantly diminished in Alb–Cre *Foxm1b*$^{-/-}$ livers (Fig. 6A). Similar levels of Cdc25C protein are found in liver extracts from Alb–Cre *Foxm1b*$^{-/-}$ and *Foxm1b* fl/fl mice after 6 wk of DEN/PB treatment (Fig. 6A). A more severe reduction in hepatic levels of Cdc25C protein was observed in *Foxm1b* fl/fl mice compared with Alb–Cre *Foxm1b*$^{-/-}$ mice, and hepatic expression of Cdc25C protein was significantly reduced in both types of mice by 33 wk of DEN/PB exposure (Fig. 6A). In contrast, hepatic expression of Cdc25B protein became undetectable in both mice by 23 wk of

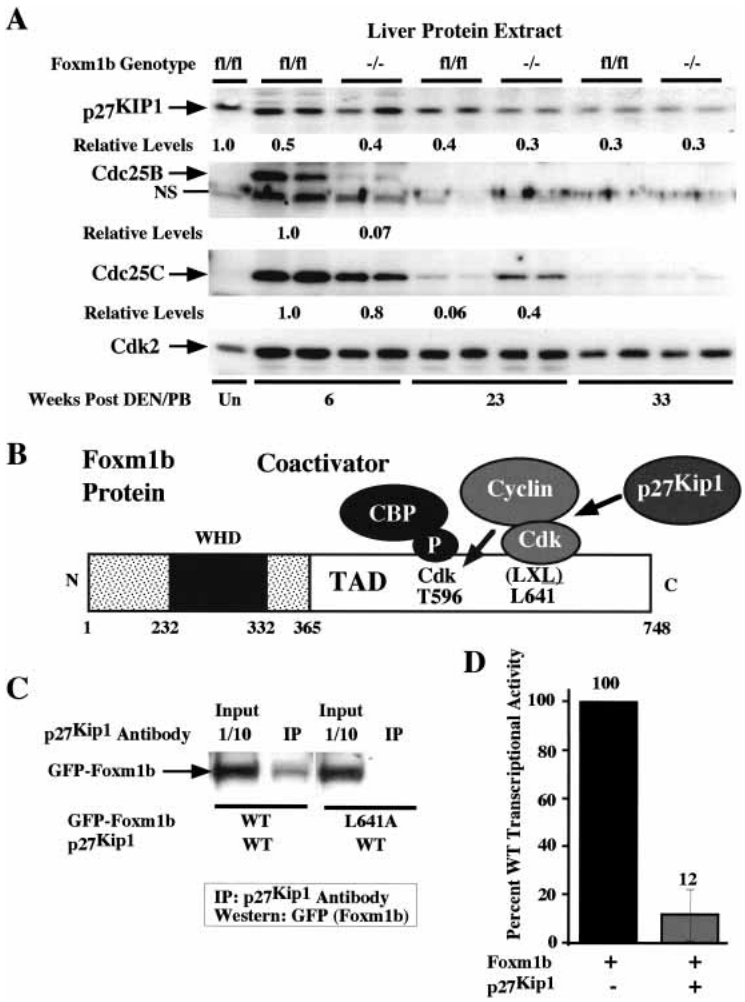

Figure 6. The Cdk inhibitor $p27^{Kip1}$ protein associates with Foxm1b through the Cdk–Cyclin complexes and inhibits its transcriptional activity. (*A*) Western blot analysis of liver protein extracts isolated from either untreated (Un) or DEN/PB-treated mice. Liver protein extracts prepared from two distinct mice following either no treatment or 6, 23, and 33 wk of DEN/PB exposure were used for Western blot analysis with antibodies specific to either $p27^{Kip1}$, Cdc25B, or Cdc25C proteins. Expression levels of Cdk2 were used as a loading control. (*B*) Drawing depicting mechanisms regulating Foxm1b transcriptional activity. Schematically shown is the Foxm1b winged helix DNA-binding domain (WHD), the C-terminal transcriptional activation domain (TAD; Ye et al. 1997), the Foxm1b LXL motif (639–641) that recruits either the Cdk2–Cyclin E/A (S phase), or Cdk1–Cyclin B (G2 phase) complexes. Foxm1b transcriptional activity requires binding of the Cdk–Cyclin complexes, which is necessary for efficient phosphorylation of the Foxm1b Cdk 596 site that recruits the CREB Binding Protein (CBP) histone acetyltransferase (Major et al. 2004). (*C*) The $p27^{Kip1}$ protein associates with GFP–Foxm1b protein through interaction with the Cdk–Cyclin complexes. We performed Co-IP assays with protein extracts prepared from U2OS cells that were transiently transfected with CMV $p27^{Kip1}$ and CMV expression vectors containing either wild-type GFP–Foxm1b or GFP–Foxm1b L641A mutant protein that fail to recruit the Cdk–Cyclin complexes. Protein extracts were immunoprecipitated with $p27^{Kip1}$ antibody followed by Western blot analysis with GFP monoclonal antibody. We included a control lane containing 1/10 of the extract used in the Co-IP experiment. (*D*) The $p27^{Kip1}$ protein inhibits Foxm1b-transcriptional activity in cotransfection assays. We transiently transfected U2OS cells with the 6× Foxm1b-TATA-luciferase reporter plasmid (Rausa et al. 2003; Major et al. 2004) and the CMV Foxm1b either with or without the CMV $p27^{Kip1}$ expression vector. Transfected cells were harvested at 48 h after transfection and processed for dual luciferase assays to determine Foxm1b transcriptional activity. Transfections were performed twice in triplicate and used to calculate the percent of wild-type Foxm1b transcriptional levels (±S.D.).

DEN/PB exposure (Fig. 6A). Taken together, our data suggested that decreased proliferation in Alb–Cre *Foxm1b*$^{-/-}$ hepatocytes is likely due to sustained nuclear levels of Cdk inhibitor $p27^{Kip1}$ protein and diminished expression of the Cdk1-activator Cdc25B.

The Cdk inhibitor $p27^{Kip1}$ protein associates with Foxm1b through the Cdk–Cyclin complexes and inhibits its transcriptional activity

Our recent studies demonstrated that Foxm1b transcriptional activity requires an LXL Cdk docking site (639–641) that recruits either the Cdk2–Cyclin E/A (S phase) or Cdk1–Cyclin B (G2 phase) complexes to the Foxm1b transcriptional activation domain (Fig. 6B), which is required for efficient phosphorylation of the Foxm1b Cdk 596 site (Major et al. 2004). Retention of this Foxm1b Cdk site at Thr 596 residue was found to be essential for transcriptional activity by mediating phosphorylation-dependent recruitment of the CREB-binding protein (CBP) histone acetyltransferase (Major et al. 2004). The fact that Foxm1b deficiency caused persistent nuclear accumulation of $p27^{Kip1}$ protein led us to investigate whether the $p27^{Kip1}$ Cdk inhibitor protein associated with the Foxm1b protein directly or indirectly through the Cdk–Cyclin complex (Fig. 6B). Protein extracts were prepared from U2OS cells that were transiently transfected with the CMV $p27^{Kip1}$ and CMV expression constructs containing either wild-type GFP–Foxm1b or the GFP–Foxm1b L641A mutant that failed to interact with the Cdk–Cyclin complexes (Major et al. 2004). These U2OS cell-transfected lysates were immunoprecipitated with the $p27^{Kip1}$ antibody, followed by Western blot analysis with GFP antibody. These coimmunoprecipitation (Co-IP) experiments demonstrated that the $p27^{Kip1}$ protein associated with the wild-type Foxm1b protein, whereas $p27^{Kip1}$ was unable to bind to the GFP–Foxm1b L641A mutant protein (Fig. 6C). These results suggested that the $p27^{Kip1}$ protein associates with the Cdk–Cyclin complexes, which are recruited by the Foxm1b transcrip-

tional activation domain through the LXL Cdk docking motif (Fig. 6B).

To determine whether the $p27^{Kip1}$ protein could inhibit Foxm1b transcriptional activity, we transiently transfected U2OS cells with the 6× Foxm1b-TATA-luciferase reporter plasmid (Rausa et al. 2003; Major et al. 2004) with the CMV wild-type Foxm1b and $p27^{Kip1}$ expression vectors. Transfected cells were harvested at 48 h after transfection and processed for dual luciferase assays to determine Foxm1b transcriptional activity. Cotransfection of $p27^{Kip1}$ expression vector caused a significant reduction in Foxm1b transcriptional activity (Fig. 6D). This finding is consistent with the ability of the $p27^{Kip1}$ protein to inhibit kinase activity of the Cdk–Cyclin complexes (Polyak et al. 1994; Zerfass-Thome et al. 1997), which are required for Foxm1b transcriptional activity through Cdk phosphorylation-dependent recruitment of the CBP coactivator protein (Major et al. 2004).

Endogenous $p19^{ARF}$ tumor suppressor associates with Foxm1b protein in liver extracts prepared from mice following 6 wk of DEN/PB exposure

The DEN/PB induction of liver tumors stimulates expression of various oncogenes (Graveel et al. 2001), and that oncogenic stress is known to induce expression of $p19^{ARF}$ (p19) tumor suppressor (Sherr and McCormick 2002). Induced protein levels of the p19 tumor suppressor are found at early time points during tumor induction, but its expression is extinguished in a variety of tumors (Sherr and McCormick 2002). Western blot analysis demonstrated that hepatic expression of p19 protein is induced at 6 wk after DEN/PB exposure, but its liver expression was significantly diminished by 23 following DEN/PB exposure (Fig. 7A), a finding consistent with those obtained with other tumors (Sherr and McCormick 2002).

The importance of Foxm1b in the proliferative expansion of liver tumors led us to investigate whether the p19 tumor suppressor protein associated with the Foxm1b protein. Co-IP assays were performed with liver protein extracts prepared from *Foxm1b* fl/fl and Alb–Cre *Foxm1b*$^{-/-}$ mice following either 6 or 23 wk of DEN/PB treatment (Fig. 7B). As a positive control, we also performed Co-IP experiments with protein extracts prepared from mouse embryo fibroblasts (MEFs) that were cultured in vitro for 12 passages to induce endogenous protein expression of the p19 tumor suppressor (Kamijo et al. 1997). The protein extracts were first immunoprecipitated with p19 antibody and then analyzed by Western blot analysis with a mouse Foxm1b antibody. These Co-IP studies demonstrated efficient association between endogenous Foxm1b and p19 proteins in extracts prepared from either *Foxm1b* fl/fl livers at 6 wk of DEN/PB exposure or late passage MEFs, but not with liver extracts from Alb–Cre *Foxm1b*$^{-/-}$ mice, which lacked hepatocyte expression of Foxm1b (Fig. 7B). Negative controls showed that Foxm1b protein failed to Co-IP with p19 in protein extracts prepared from *Foxm1b* fl/fl livers at 23 wk of DEN/PB treatment, which no longer express the p19 protein, but continue to express Foxm1b protein (Figs. 7B, 3C).

The $p19^{ARF}$ 26–44 sequences are sufficient to associate with and inhibit Foxm1b transcriptional activity

To identify $p19^{ARF}$ protein sequences that are essential for association with Foxm1b protein, we performed Co-IP assays with protein extracts prepared from transiently transfected U2OS cells, which lack endogenous expression of the $p19^{ARF}$ tumor-suppressor protein (Martelli et al. 2001). U2OS cells were cotransfected with CMV GFP–Foxm1b expression vector and CMV expression plasmids containing either wild-type $p19^{ARF}$ protein or N-terminal deletion mutants of the $p19^{ARF}$ protein (Δ1–14, Δ15–25, Δ26–37, or Δ26–37 + Δ1–14) that were fused to the HA epitope tag (Weber et al. 2000). Protein extracts were incubated with HA antibody to immunoprecipitate the HA-$p19^{ARF}$ protein, followed by Western blot analysis with a monoclonal antibody specific to GFP protein to detect the GFP–FoxM1B fusion protein. These Co-IP experiments demonstrated that the N-terminal 25 amino acid residues of the $p19^{ARF}$ (p19) protein were dispensable for association with the GFP–Foxm1b protein (Fig. 7C,D). In contrast, the p19 amino acid residues 26–37 were essential for association with the GFP–Foxm1b fusion protein (Fig. 7C,D). Furthermore, retention of the C-terminal 60 amino acids from the Foxm1b protein (688–748) was required for p19 protein binding (Fig. 7C,D). To identify p19 protein sequences that are sufficient for association with Foxm1b protein, we performed Co-IP assays with protein extracts prepared from U2OS cells that were transiently transfected with CMV GFP–Foxm1b expression plasmid and the CMV expression vector containing the V5 epitope tagged $p19^{ARF}$ 26–44 or $p19^{ARF}$ 26–55 sequences. At the N terminus of either the $p19^{ARF}$ sequences 26–44 or 26–55, we placed the protein transduction/nuclear localization domain (MGYGRKKRRQRRR) from the HIV–TAT protein (Becker-Hapak et al. 2001). Protein extracts were incubated with the V5 epitope tag antibody to immunoprecipitate the p19 protein, followed by Western blot analysis with GFP monoclonal antibody to detect the GFP–FoxM1B fusion protein. These Co-IP experiments demonstrated that p19 amino acid residues 26–44 were sufficient to associate with the Foxm1b protein (Fig. 7E).

To determine whether formation of the p19–FoxM1B protein complex could effectively inhibit Foxm1b transcriptional activity, we transiently transfected U2OS cells with the 6× Foxm1b-TATA-luciferase reporter plasmid (Rausa et al. 2003; Major et al. 2004) and the CMV wild-type Foxm1b and p19 expression vectors (Fig. 7F). These cotransfection assays demonstrated that both wild-type p19 and mutant T7-$p19^{ARF}$Δ1–14, T7-$p19^{ARF}$Δ15–25, V5-TAT-$p19^{ARF}$ 26–44, and V5-TAT-$p19^{ARF}$ 26–55 proteins that retained their ability to associate with Foxm1b protein (Fig. 7D,E) were able to significantly decrease Foxm1b transcriptional activity (Fig. 7F). In contrast, the T7-$p19^{ARF}$Δ26–37 proteins, which

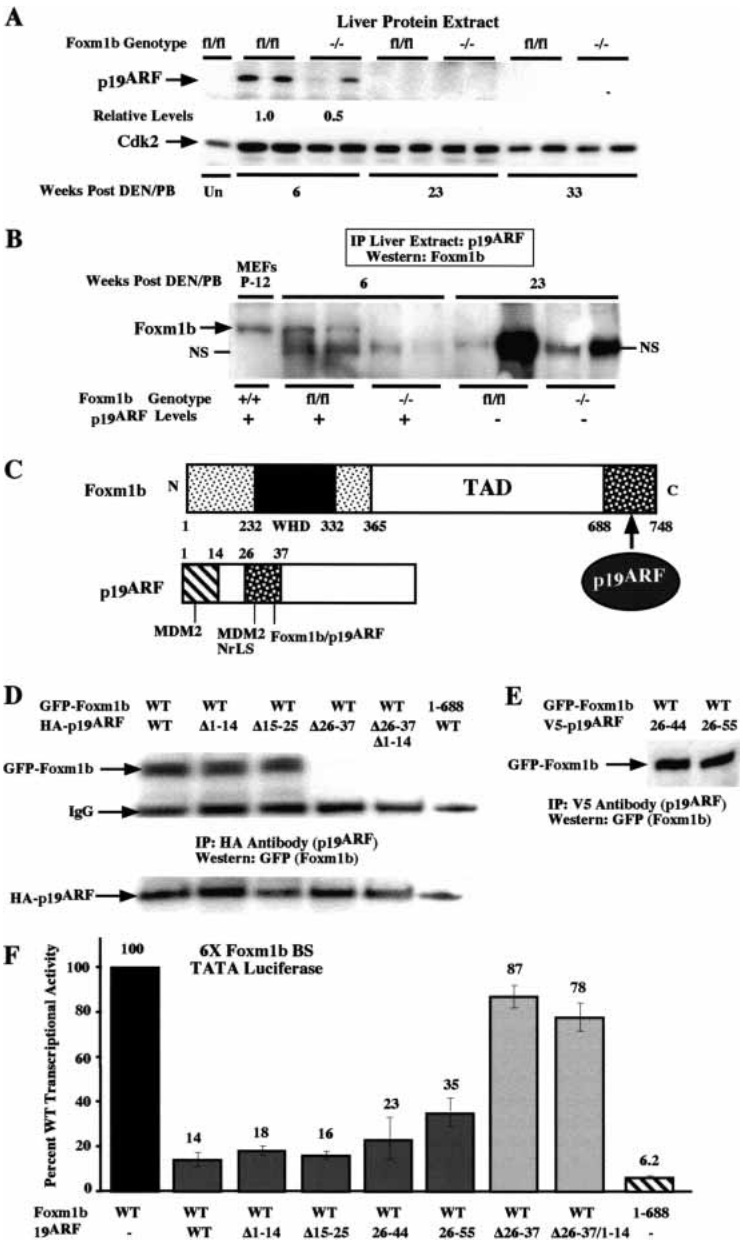

Figure 7. p19^{ARF} tumor suppressor associates with Foxm1b in liver protein extracts and the p19^{ARF} 26–44 sequences are sufficient to inhibit Foxm1b transcriptional activity. (*A*) Expression of p19^{ARF} tumor suppressor is transiently induced after 6 wk of DEN/PB exposure. We performed Western Blot analysis with liver extracts prepared from two distinct mice following either no treatment (Un) or 6, 23, and 33 wk of DEN/PB exposure with a p19^{ARF} (p19) antibody. Expression levels of Cdk2 were used as a loading control. (*B*) p19^{ARF} protein associates with endogenous Foxm1b protein in liver extracts from mice treated for 6 wk with DEN/PB. Co-IP assays were performed with liver protein extracts prepared from *Foxm1b* fl/fl and Alb–Cre *Foxm1b*$^{-/-}$ mice following either 6 or 23 wk of DEN/PB treatment. As a positive control, we also performed Co-IP experiments with protein extracts prepared from mouse embryo fibroblasts (MEFs) that were cultured in vitro for 12 passages to induce endogenous protein expression of the p19 tumor suppressor (Kamijo et al. 1997). The protein extracts were first immunoprecipitated with p19 antibody and then analyzed by Western blot analysis with a mouse Foxm1b antibody. (*C*) Drawing depicting functional domains of the Foxm1b and p19^{ARF} tumor suppressor proteins. Schematically shown is the Foxm1b winged helix DNA-binding domain (WHD), the C-terminal transcriptional activation domain (TAD; Ye et al. 1997), and the C-terminal region (688–748) required for p19^{ARF} (p19) binding. Schematically shown are the p19 nucleolar localization sequence (NrLS) and the p19 Mdm2 and Foxm1b-binding sites (Weber et al. 2000). (*D*) p19^{ARF} 26–37 and Foxm1b 688–748 residues are essential for protein association. To identify p19 protein sequences that are essential for association with Foxm1b protein, we performed Co-IP assays with protein extracts prepared from U2OS cells that were transiently transfected with CMV green fluorescent protein (GFP) Foxm1b fusion protein and with p19 expression vectors. These included expression vectors containing either wild-type p19 protein or N-terminal deletion mutants of the p19 protein (Δ1–14, Δ15–25, Δ26–37, Δ26–37 + Δ1–14) that were fused with an HA epitope tag (Weber et al. 2000). The p19 protein was immunoprecipitated from transfected protein extracts with HA antibody, followed by Western blot analysis with a monoclonal antibody specific to the GFP protein to detect the GFP–Foxm1b fusion protein. (*E*) The p19^{ARF} sequences 26–44 are sufficient to interact with Foxm1b protein. To identify p19 protein sequences that are sufficient for association with Foxm1b protein, we performed Co-IP assays with protein extracts prepared from U2OS cells that were transiently transfected with CMV GFP–Foxm1b fusion protein and expression vector containing V5 epitope tagged p19^{ARF} 26–44 or p19^{ARF} 26–55 sequences (see Materials and Methods). The p19 protein was immunoprecipitated from transfected protein extracts with V5 epitope antibody, followed by Western blot analysis with GFP monoclonal antibody. (*F*) The p19 protein inhibits Foxm1b transcriptional activity in cotransfection assays. We transiently transfected U2OS cells with the 6× Foxm1b-TATA-luciferase reporter plasmid (Rausa et al. 2003; Major et al. 2004) and the CMV Foxm1b wild type (1–748) and with either CMV wild-type p19 or the indicated N-terminal mutant T7-p19 or V5-p19 26–44 or 26–55 expression vector. We also performed transfection with CMV Foxm1b (1–688) that removed 60 amino acids from the C terminus. Transfected cells were harvested at 48 h after transfection and processed for dual luciferase assays to determine Foxm1b transcriptional activity as described in the legend for Figure 6D.

no longer associated with the Foxm1b protein (Fig. 7D) were unable to significantly reduce Foxm1b transcriptional activity in these cotransfection assays (Fig. 7F). Interestingly, deletion of the Foxm1b C-terminal sequences required for association with p19 protein (Fig. 7D; Foxm1b 1–688) was also found to be essential for Foxm1b transcriptional activity (Fig. 7F). These studies enabled us to identify the Foxm1b transcription factor as a novel inhibitory target for the p19^{ARF} tumor suppressor, a finding consistent with the important role of Foxm1b in proliferative expansion during liver tumor progression.

The p19^{ARF} tumor suppressor targets Foxm1b protein to the nucleolus

Cotransfection assays demonstrated that the p19^{ARF} (p19) protein targets the E2F transcription factor to the nucleolus, and thus provides an additional mechanism by which to limit progression into S phase (Martelli et al. 2001; Datta et al. 2002). Consistent with the E2F studies, U2OS cell cotransfection studies demonstrated that HA-tagged p19 was able to target GFP–Foxm1b fusion protein to the nucleolus (Fig. 8A–C). Whereas GFP–Foxm1b 1–748 full-length protein exhibited nuclear staining (Fig. 8D), nucleolar targeting of GFP–Foxm1b fusion protein was found in cotransfections with expression vectors containing either wild-type p19 or mutant p19 proteins that were still able to associate with Foxm1b protein (Fig. 8E,F). Published studies have shown that residues 26–37 of the p19 protein contained the nucleolar localization sequence (NrLS) and the second Mdm2-binding sequence (Weber et al. 2000). Consistent with these studies, the GFP–Foxm1b protein was targeted to the nucleolus by expression vectors containing either the V5-TAT-p19^{ARF} 26–44 or V5-TAT-p19^{ARF} 26–55 sequences (Fig. 8G,H), and these p19 sequences were also localized to the nucleolus (Fig. 8I; data not shown). In contrast, nuclear fluorescence was found with the GFP–Foxm1b wild-type protein that was transfected with the CMV p19^{ARF}Δ26–37 mutant that failed to associate with Foxm1b protein (Fig. 8J). Likewise, cotransfection assays with the CMV wild-type p19 and CMV GFP–Foxm1b 1–688 expression vectors showed nuclear fluorescence of the mutant GFP–Foxm1b 1–688 protein, a finding consistent with this Foxm1b mutant's inability to associate with the p19 protein (Figs. 8K, 7D). These studies suggest that association between the p19 tumor suppressor and Foxm1b results in targeting Foxm1b to the nucleolus and Foxm1b transcriptional inhibition.

A membrane-transducing (D-Arg)$_9$ p19^{ARF} 26–44 peptide significantly reduces both Foxm1b transcriptional activity and Foxm1b-induced cell colony formation on soft agar

Published studies demonstrate that addition of nine D-Arg to the N terminus of polypeptides significantly enhances their cellular uptake compared with the protein

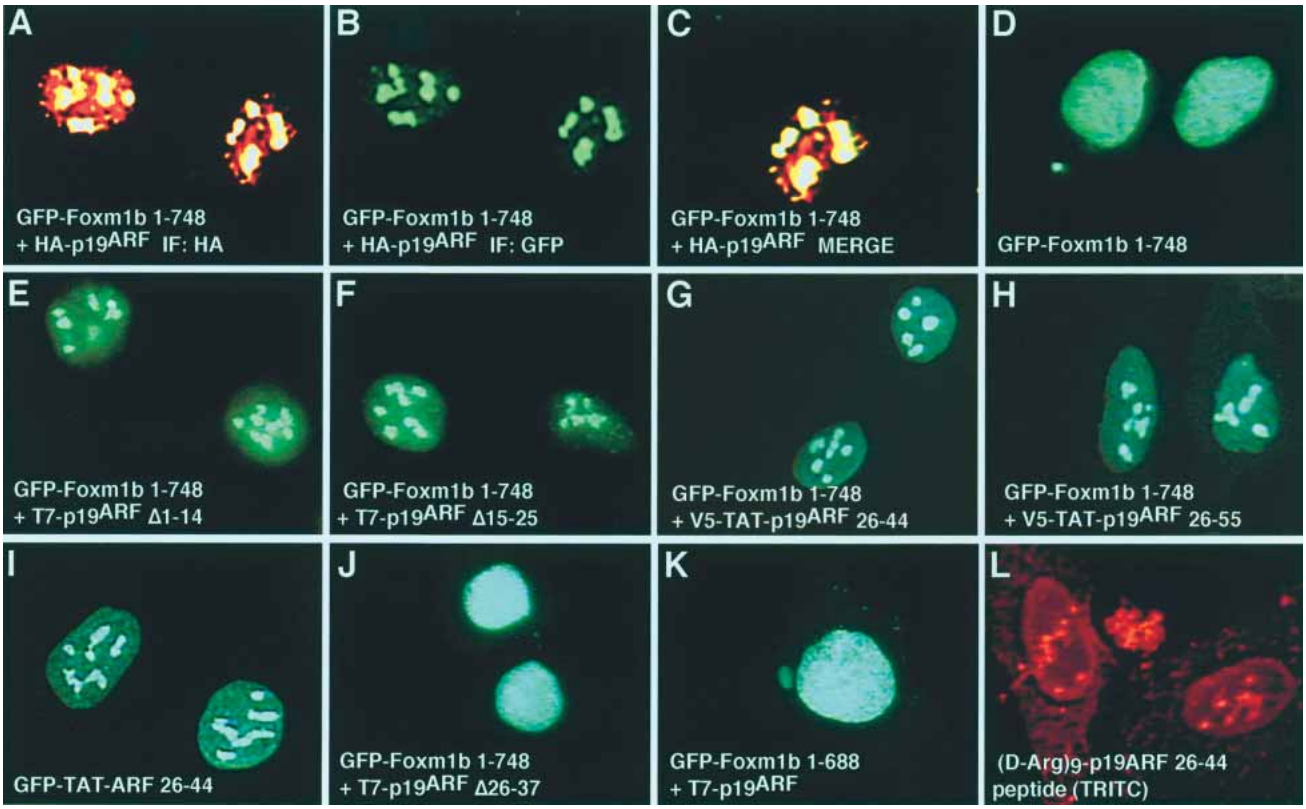

Figure 8. The p19^{ARF} tumor suppressor targets Foxm1b protein to the nucleolus. (*A–D*) U2OS cells were transfected with HA-p19ARF and GFP–Foxm1b expression vectors, demonstrating that the HA-tagged p19 (*A*) was able to target nuclear fluorescence of wild-type GFP–Foxm1b fusion protein (*D*) to the nucleolus (*B*,*C*). (*E–H*) Nucleolar targeting of GFP–Foxm1b wild-type protein was found in cotransfections with CMV expression vectors containing mutant p19^{ARF} proteins (Δ1–14, Δ15–25, 26–44, or 26–55) that were still able to associate with Foxm1b protein. (*I*) Nucleolar fluorescence was found with CMV GFP–p19^{ARF} 26–44 or GFP– p19^{ARF} 26–55 proteins. (*J*) Nuclear fluorescence was found with CMV wild-type GFP–Foxm1b and expression vector containing mutant p19^{ARF}Δ26–37 protein that failed to interact with Foxm1b. (*K*) Transfection of CMV wild-type p19 expression vector was unable to elicit nucleolar targeting of GFP–Foxm1b 1–688 protein, which failed to bind to p19 protein. (*L*) Treatment of U2OS cells for 24 h with the TRITC fluorescently tagged (D-Arg)$_9$-p19^{ARF} 26–44 peptide demonstrated that this p19^{ARF} peptide is transduced into the cell and is localized to the nucleolus.

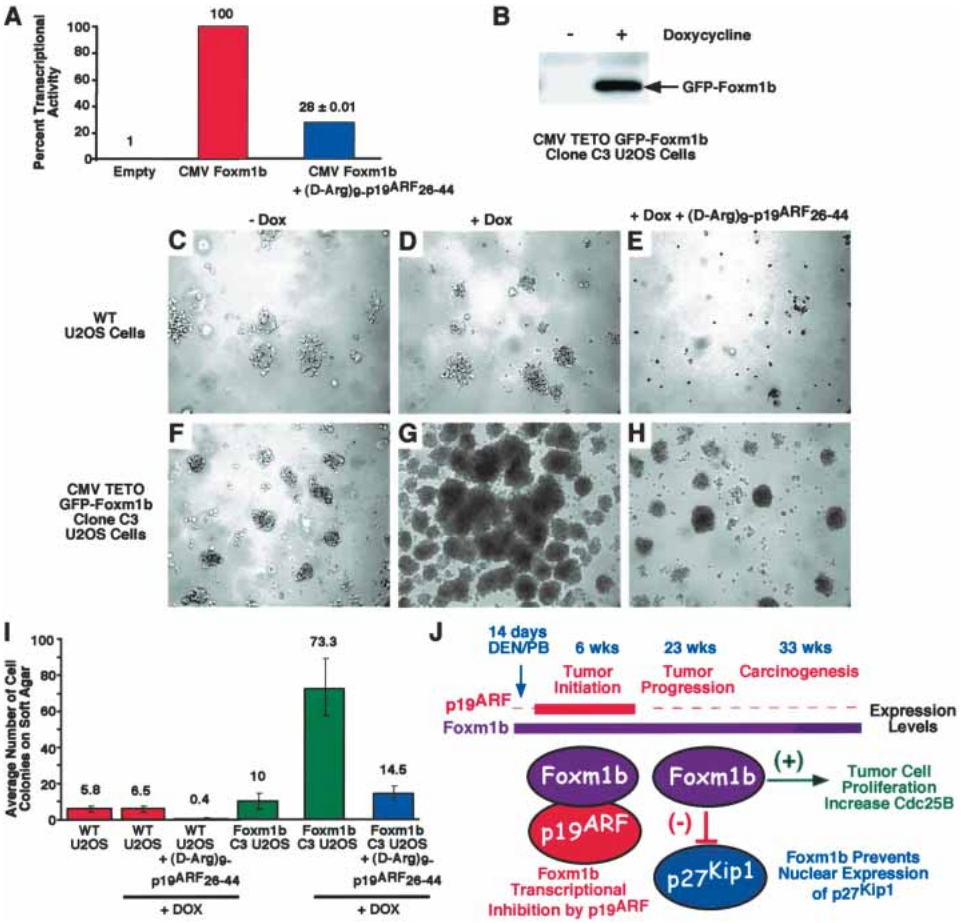

Figure 9. A membrane-transducing $(D\text{-}Arg)_9$ $p19^{ARF}$ 26–44 peptide significantly reduces both Foxm1b transcriptional activity and Foxm1b-induced cell colony formation on soft agar. (*A*) The $(D\text{-}Arg)_9$-$p19^{ARF}$ 26–44 peptide is an effective inhibitor of Foxm1b transcriptional activity. Treatment of U2OS cells with 12 µM of the $(D\text{-}Arg)_9$-$p19^{ARF}$ 26–44 peptide that were transfected with CMV-Foxm1b expression vector and the 6× Foxm1b-TATA-luciferase plasmid resulted in significant reduction in Foxm1b transcriptional activation of its target reporter gene. Transfected cells were harvested at 48 h after transfection and processed for dual luciferase assays to determine Foxm1b transcriptional activity as described in the legend for Figure 6D. (*B*) The CMV-TETO GFP–Foxm1b U2OS clone C3 cell line displayed Doxycycline-inducible expression of the GFP–Foxm1b fusion protein. We used the tetracycline (TET)-regulated T-REx System (Yao et al. 1998) to produce the U2OS Clone 3 cell line as described in Materials and Methods, which induces intermediate levels of the GFP–Foxm1b protein in response to Doxycycline treatment. (*C–H*) The $(D\text{-}Arg)_9$-$p19^{ARF}$ 26–44 peptide significantly diminished the ability of induced GFP–Foxm1b to stimulate colony formation of the U2OS clone C3 cells on soft agar. Doxycycline induced Foxm1b–GFP expression stimulates anchorage-independent growth in the U2OS clone C3 cell line (*F,G*) as assessed by propagation for 2 wk on soft agar (Conzen et al. 2000), whereas the $(D\text{-}Arg)_9$-$p19^{ARF}$ 26–44 peptide significantly inhibited colony formation of U2OS cells on soft agar (*E,H*). (*I*) Quantitation of Foxm1b-induced formation of U2OS cell colonies on soft agar treated or not treated with the $(D\text{-}Arg)_9$-$p19^{ARF}$ 26–44 peptide. We counted the number of U2OS colonies of the indicated treatments from four to five different 100× fields and determined the mean number of cell colonies (±S.D.). (*J*) Model for Foxm1b transcriptional inhibition by p19ARF protein during liver tumor initiation, progression, and carcinogenesis in response to DEN/PB liver tumor induction. Foxm1b protein diminishes nuclear expression of the Cdk inhibitor $p27^{Kip1}$ protein and regulating expression of Cdk-1 regulator Cdc25B phosphatase.

transduction/nuclear localization domain from the HIV–TAT protein (Wender et al. 2000). We therefore synthesized a $p19^{ARF}$ 26–44 peptide containing nine D-Arg residues at the N terminus (Wender et al. 2000) that is fluorescently tagged with Lissamine (TRITC) on the N terminus and acetylated at the C terminus. Treatment of U2OS cells with 12 µM of the $(D\text{-}Arg)_9$-$p19^{ARF}$ 26–44 peptide (rrrrrrrrrKFVRSRRPRTASCALAFVN) for 24 h demonstrated that this $(D\text{-}Arg)_9$-$p19^{ARF}$ 26–44 peptide is efficiently transduced into all of the cells, and that its fluorescence localizes to the nucleolus (Fig. 8L; data not shown). Furthermore, exposure of U2OS cells with 12 µM of the $(D\text{-}Arg)_9$-$p19^{ARF}$ 26–44 peptide for 7 d caused neither toxicity nor any increases in apoptosis (data not shown). Furthermore, treatment of U2OS cells with 12 µM of the $(D\text{-}Arg)_9$-$p19^{ARF}$ 26–44 peptide that were transfected with CMV-Foxm1b expression vector, and the 6× Foxm1b-TATA-luciferase plasmid resulted in significant reduction in Foxm1b transcriptional activity (Fig. 9A), suggesting that this $p19^{ARF}$ peptide is

an effective inhibitor of Foxm1b transcriptional activity.

We next wanted to determine whether conditional overexpression of Foxm1b protein could enhance anchorage-independent growth of U2OS cells. We used tetracycline (TET)-regulated T-REx System (Yao et al. 1998) to conditionally express the GFP–Foxm1b protein in U2OS cells. We transfected the CMV-TETO GFP–Foxm1b expression plasmid into T-REx-U2OS cells (contains TET repressor) and selected clonal U2OS cell lines that are doxycycline inducible for GFP–Foxm1b expression. In response to doxycycline treatment, the CMV-TETO GFP–Foxm1b U2OS clone C3 cell line induced intermediate levels of GFP–Foxm1b fusion protein (Fig. 9B). We therefore selected the U2OS clone C3 cell line to examine whether doxycycline-induced expression of Foxm1b–GFP protein would enhance anchorage-independent growth as assessed by propagation for 2 wk on soft agar (Conzen et al. 2000). These soft agar experiments demonstrated that induced expression of GFP–Foxm1b protein caused a significant increase in anchorage-independent growth, as evidenced by increasing the number and size of U2OS cell colonies on soft agar (Fig. 9G,I) compared with uninduced controls (Fig. 9F) or the wild-type U2OS cells (Fig. 9C,D). These results suggest that the Foxm1b protein displayed oncogenic properties by stimulating anchorage-independent growth of U2OS cell colonies on soft agar. To determine whether the $(D\text{-}Arg)_9$-$p19^{ARF}$ 26–44 peptide could inhibit this Foxm1b-induced colony formation of U2OS cells on soft agar, we treated the doxycycline-induced U2OS clone 3 cells with 12 μM of the $(D\text{-}Arg)_9$-$p19^{ARF}$ 26–44 peptide 1 d prior to plating and continued to add this concentration of $(D\text{-}Arg)_9$-$p19^{ARF}$ 26–44 peptide in the soft agar and growth medium throughout the duration of the experiment (see Materials and Methods). The results of these soft agar studies demonstrated that the $(D\text{-}Arg)_9$-$p19^{ARF}$ 26–44 peptide significantly diminished the ability of induced GFP–Foxm1b to stimulate colony formation of the U2OS clone C3 cells on soft agar (Fig. 9H,I). Furthermore, the $(D\text{-}Arg)_9$-$p19^{ARF}$ 26–44 peptide significantly diminished the ability of the parental U2OS cells to form colonies on soft agar (Fig. 9E,I). Taken together, these studies suggests that the $(D\text{-}Arg)_9$-$p19^{ARF}$ 26–44 peptide is an effective inhibitor of both Foxm1b-mediated transcriptional activation and Foxm1b-induced stimulation in anchorage-independent growth that is required for cellular transformation.

Discussion

Liver regeneration studies with genetically altered mice that either prematurely expressed Foxm1b in hepatocytes (Ye et al. 1999; Wang et al. 2001a,b) or contained a hepatocyte-specific deletion of the *Foxm1b* fl/fl targeted allele (Wang et al. 2002a; Costa et al. 2003) demonstrated that Foxm1b is required for hepatocyte proliferation through controlling levels of cell cycle regulatory proteins. Microarray analysis of HCC tumors demonstrated that expression of Foxm1b (Foxm1) was increased in HCC (Okabe et al. 2001), but whether Foxm1b transcriptional activity is essential for development of HCC remained to be determined. Here, we demonstrated that both male and female Alb–Cre *Foxm1b*$^{-/-}$ livers are highly resistant to developing HCC tumors in response to DEN/PB exposure, an established method for induction of numerous HCC tumors in mouse liver (Tamano et al. 1994; Sargent et al. 1996; Kalinina et al. 2003). We showed that Alb–Cre *Foxm1b*$^{-/-}$ hepatocytes express the GST-pi protein, a marker for altered enzyme foci in response to DEN/PB exposure (Hatayama et al. 1993). However, these Alb–Cre *Foxm1b*$^{-/-}$ hepatocytes failed to undergo extensive proliferation following DEN/PB exposure required for liver tumor progression and was associated with nuclear accumulation of the Cdk inhibitor $p27^{Kip1}$ protein and significantly reduced levels of the Cdc25B phosphatase (Fig. 9J). Moreover, the fact that Foxm1b is expressed in numerous tumor cell lines (Korver et al. 1997; Yao et al. 1997; Ye et al. 1997), in basal cell carcinomas (Teh et al. 2002) and in anaplastic astrocytomas and glioblastomas (van den Boom et al. 2003), suggests that Foxm1b is likely required for proliferative expansion of many different tumors.

We also showed that the $p19^{ARF}$ residues 26–44 were sufficient to bind to the Foxm1b protein (Fig. 7E), inhibit Foxm1b transcriptional activity (Fig. 7F), and target Foxm1b protein to the nucleolus (Fig. 8G). Conditional overexpression of Foxm1b protein in osteosarcoma U2OS cells stimulated anchorage-independent growth of U2OS cells on soft agar (Fig. 9B,F,G), suggesting that increase levels of Foxm1b are involved in oncogenic transformation. We demonstrated that a $p19^{ARF}$ 26–44 peptide containing nine D-Arg, to enhance cellular uptake of peptide (Wender et al. 2000), efficiently transduced into cells, localized to the nucleolus (Fig. 8L), and significantly reduced Foxm1b transcriptional activity (Fig. 9A). Furthermore, this $(D\text{-}Arg)_9$-$p19^{ARF}$ 26–44 was sufficient to cause significant reduction in Foxm1b-induced stimulation of anchorage-independent growth of U2OS cell colonies on soft agar without displaying cellular toxicity (Fig. 9G–I). Our studies demonstrated that the $(D\text{-}Arg)_9$-$p19^{ARF}$ 26–44 peptide is an effective inhibitor of Foxm1b function that may be useful for HCC therapy.

Sustained nuclear levels of $p27^{Kip1}$ protein in Alb–Cre *Foxm1b*$^{-/-}$ hepatocytes is likely contributing to diminished cellular proliferation necessary for tumor cell progression, because $p27^{Kip1}$ protein prevents Cdk phosphorylation of RB protein required for activation of E2F transcription factors (Sherr and Roberts 1999). An increase in the number of polyploid hepatocytes was also observed in TTR- $p21^{Cip1}$ TG mice that ectopically expressed the related Cdk inhibitor $p21^{Cip1}$ protein in hepatocytes (Wu et al. 1996). Consistent with these findings, our current studies found persistent nuclear accumulation of $p27^{Kip1}$ protein only in regenerating Alb–Cre *Foxm1b*$^{-/-}$ hepatocytes (Fig. 5A,B). Despite high levels of nuclear $p27^{Kip1}$ protein, these Alb–Cre *Foxm1b*$^{-/-}$ hepatocytes exhibited detectable BrdU incorporation rates that were 50% of those found in *Foxm1b* fl/fl livers at 36 h after PHx, but they failed to progress into mitosis (Wang et al. 2002a). Our data suggested that *Foxm1b*-

deficient hepatocytes became more polyploid than control hepatocytes at 23 and 33 wk of DEN/PB treatment without notable changes in hepatocyte function as assessed by serum analysis. On the basis of these studies, sustained hepatocyte levels of nuclear $p27^{Kip1}$ protein and diminished Cdc25B protein found in Alb–Cre *Foxm1b*$^{-/-}$ hepatocytes after DEN/PB exposure is likely contributing to low levels of hepatocyte DNA replication with a block in progression into mitosis leading to an increase in hepatocyte ploidy. These results are consistent with low levels of hepatocyte DNA replication with a significant reduction in mitosis as was previously found in *Foxm1b*-deficient hepatocytes during liver regeneration and development (Korver et al. 1998; Wang et al. 2002a).

Persistent hepatocyte levels of nuclear $p27^{Kip1}$ protein were associated with the resistance of Alb–Cre *Foxm1b*$^{-/-}$ mice to developing liver tumors after 23 or 33 wk of DEN/PB exposure. In contrast, significant reduction in hepatocyte nuclear levels of $p27^{Kip1}$ protein was found in *Foxm1b* fl/fl control mice at 6, 23, and 33 wk after DEN/PB treatment, and this reduction was associated with development of both hepatic adenomas and HCC. All nine female Alb–Cre *Foxm1b*$^{-/-}$ livers were devoid of tumors following 50 wk of DEN/PB exposure, and they continued to exhibit hepatocyte nuclear levels of $p27^{Kip1}$ protein (Fig. 5K,N). After 50 wk of DEN/PB exposure, we found that significant decreases in nuclear levels of $p27^{Kip1}$ protein of male Alb–Cre *Foxm1b*$^{-/-}$ hepatocytes, which correlate with the 50% increase in liver tumor incidence (Fig. 5L,N). These results suggested that the diminished nuclear expression of $p27^{Kip1}$ protein in male Alb–Cre *Foxm1b*$^{-/-}$ livers contributed to increased development of liver tumors after this prolonged DEN/PB treatment. In support of these findings, diminished nuclear localization of the $p27^{Kip1}$ protein was associated with more aggressive tumors in human breast cancer (Porter et al. 1997; Liang et al. 2002; Shin et al. 2002; Viglietto et al. 2002; Alkarain and Slingerland 2004).

We found that Alb–Cre *Foxm1b*$^{-/-}$ livers did not exhibit increased expression of total $p27^{Kip1}$ protein, but rather, that *Foxm1b* deficiency resulted in increased hepatocyte levels of nuclear $p27^{Kip1}$ protein following DEN/PB exposure (Figs. 5, 6). Consistent with this hypothesis, diminished hepatocyte levels of nuclear $p27^{kip1}$ protein were found in regenerating livers of old-aged mice when Foxm1b expression was restored by infection with an Adenovirus Foxm1b expression vector or by growth hormone treatment (Wang et al. 2002b; Krupczak-Hollis et al. 2003). Furthermore, we found that regenerating Foxm1b$^{-/-}$ hepatocytes failed to reduce nuclear levels of $p27^{kip1}$ protein, suggesting that Foxm1b regulates nuclear localization of the $p27^{kip1}$ protein. Our recent studies demonstrated that Foxm1b transcriptional activity requires an LXL Cdk docking motif (639–641) that recruits either the Cdk2–Cyclin E/A (S phase) or Cdk1–Cyclin B (G2 phase) complexes to the Foxm1b activation domain (Major et al. 2004). Recruitment of Cdk–cyclin complexes to the Foxm1b activation domain is necessary for efficient phosphorylation of the Cdk site at Thr residue 596 (Major et al. 2004). Retention of this Foxm1b 596 Cdk site was found to be essential for transcriptional activity by mediating Cdk phosphorylation-dependent recruitment of the CBP coactivator protein (Major et al. 2004). In this study, we showed that association between $p27^{Kip1}$ and Foxm1b proteins was dependent on retention of the Foxm1b LXL Cdk docking motif, suggesting that the $p27^{Kip1}$ protein indirectly associated with the Foxm1b protein through the Cdk–cyclin complexes. Furthermore, we showed that $p27^{Kip1}$ protein effectively inhibits Foxm1b transcriptional activity (Fig. 6), a finding consistent with the ability of the $p27^{Kip1}$ protein to inhibit kinase activity of the Cdk–Cyclin complexes (Polyak et al. 1994; Zerfass-Thome et al. 1997) that are required for Foxm1b transcriptional function (Major et al. 2004). It is therefore possible that the complex between $p27^{Kip1}$ and Foxm1b proteins may play a role in mediating diminished nuclear levels of $p27^{Kip1}$ protein. On the basis of these studies, we hypothesize that an increase in Foxm1b expression is necessary to diminish nuclear levels of $p27^{Kip1}$ protein either directly or indirectly, which is required for hepatocyte proliferation during liver tumor progression.

Diminished hepatocyte DNA replication in regenerating Alb–Cre *Foxm1b*$^{-/-}$ livers was associated with increased nuclear levels of the Cdk inhibitor $p21^{Cip1}$ protein (Wang et al. 2002a). Immunostaining of liver sections demonstrated that nuclear expression of $p21^{Cip1}$ protein in Alb–Cre *Foxm1b*$^{-/-}$ and *Foxm1b* fl/fl hepatocytes was similar and restricted to hepatocytes surrounding the central vein after 6, 23, or 33 wk of DEN/PB treatment (data not shown). This similar expression pattern of nuclear $p21^{Cip1}$ protein in hepatocytes of DEN/PB-treated mice suggested that elevated $p21^{Cip1}$ protein levels are unlikely to be involved in suppressing tumor formation in Alb–Cre *Foxm1b*$^{-/-}$ livers.

Our studies also demonstrated that Foxm1b is a novel target for transcriptional inhibition by the $p19^{ARF}$ (p19) tumor suppressor, a finding consistent with the important role of Foxm1b in the proliferative expansion of liver tumors. We found that hepatic expression of p19 protein is induced in liver extracts of control mice at 6 wk following DEN/PB exposure, and that p19 associated with Foxm1b protein in these liver protein extracts (Fig. 7A,B). In a manner similar to that observed with the E2F1 transcription factor (Martelli et al. 2001; Datta et al. 2002), we find that the p19 protein inhibits Foxm1b transcriptional activity in cotransfection assays, and that p19 protein targeted Foxm1b protein to the nucleolus. Consistent with the hypothesis that p19 negatively regulates Foxm1b transcriptional activity to diminish hepatocyte proliferation during tumorigenesis, we found that periportal control hepatocytes displayed abundant nuclear staining of the Foxm1b protein at 6 wk following DEN/PB exposure, but these hepatocytes only displayed low levels of proliferation. Increased hepatocyte levels of nuclear Foxm1b transgene protein without an increase in hepatocyte PCNA staining were also found at early time points following DEN treatment of TTR-Foxm1b TG mice (Kalinina et al. 2003). We propose that the tran-

sient induction of p19 protein levels may be involved in reducing Foxm1b activity and preventing hepatocyte proliferation early in the process of DEN/PB tumor promotion (Fig. 9J). Consistent with this hypothesis, we demonstrated that Foxm1b protein is found in the nucleolar compartment of hepatocyte nuclei following 6 wk of DEN/PB treatment, whereas Foxm1b immunostaining was excluded from the hepatocyte nucleolus after 23 wk of DEN/PB exposure, when they no longer express p19 (data not shown). In a manner congruent with other tumor studies (Sherr and McCormick 2002), hepatic levels of p19 protein are extinguished during tumor promotion at 23 wk following DEN/PB treatment, and therefore, can no longer inhibit Foxm1b ability to stimulate tumor cell proliferation at these later stages of tumorigenesis (Fig. 9J). Interestingly, elevated hepatocyte levels of Foxm1b in TTR-Foxm1b TG mice caused an increase in the size of preneoplastic and early neoplastic lesions after 23 wk DEN/PB exposure, but did not influence the incidence of HCC tumors after 33 wk of DEN/PB treatment (Kalinina et al. 2003). These results are consistent with the fact that hepatic adenomas and HCC already express ample levels of nuclear Foxm1b protein and no longer express p19 tumor suppressor, which functions to inhibit Foxm1b transcriptional activity (Fig. 9J). The Foxm1b transcription factor is therefore a potential target for inhibition by the p19 tumor suppressor, thus identifying a new pathway targeted by p19 to prevent tumor formation.

Patients with HCC tumors have poor prognoses, because late detection of these liver tumors renders current cancer therapy ineffective (Block et al. 2003; Varela et al. 2003). One of the potentially curative approaches in HCC therapy is based on interfering with HCC progression by blocking cell division. Our studies demonstrate for the first time that the Foxm1b transcription factor is required for the proliferative expansion necessary for tumor progression and constitutes a novel target in treatment of human HCC tumors. Furthermore, they suggest the possibility that restoring p19 expression may be an effective method of inhibiting Foxm1b transcriptional activity, thereby limiting the proliferative expansion of tumor cells (Fig. 9J). Our functional studies demonstrated that $p19^{ARF}$ residues 26–44 were sufficient to inhibit Foxm1b transcriptional activity and target it to the nucleolus. Consistent with this hypothesis, we demonstrated that the membrane transducing $(D\text{-}Arg)_9$-$p19^{ARF}$ 26–44 peptide significantly reduce both Foxm1b transcriptional activity and Foxm1b-induced stimulation of anchorage-independent growth, demonstrating that the $(D\text{-}Arg)_9$-$p19^{ARF}$ 26–44 peptide is an effective inhibitor of Foxm1b function that may be potentially used for HCC therapy. Furthermore, these $p19^{ARF}$ 26–44 sequences are distinct for the inhibition of Foxm1b transcriptional activity. These $p19^{ARF}$ sequences do not completely overlap with those required for inhibition of the p53 regulatory protein Mdm2 ($p19^{ARF}$ 1–14 and 26–37; Weber et al. 2000) or the proliferation-specific E2F1 transcription factor protein ($p19^{ARF}$ 6–10 and 21–25; A. Datta and P. Raychaudhuri, unpubl.).

Although targeted mutations of other proliferation-specific transcription factors were shown to delay or reduce the size of tumors, none of these transcription factors had the profound effect on proliferative expansion of tumors observed with *Foxm1b* deficiency. Using the DEN/PB liver tumor induction protocol, hepatocyte-specific deletion of the *c-Jun* transcription factor was sufficient to delay formation of hepatic adenomas, because c-Jun function is required to inhibit p53-mediated apoptosis at early stages of liver tumor progression (Eferl et al. 2003). However, *c-Jun* deficiency had no effect on incidence of HCC that were induced at later time points after DEN/PB treatment, suggesting that c-Jun's cell survival function was circumvented by secondary mutations during formation of HCC (Eferl et al. 2003). Unlike the initial resistance of *c-Jun*$^{-/-}$ livers to adenomas, *Foxm1b* deficiency did not cause an increase in apoptosis during liver tumor progression, but rather had a profound effect on the proliferative expansion of tumor cells. A TG mouse brain tumor model was developed in which RB was inactivated by expression of N-terminal fragment of SV40 T antigen (TgT_{121}) in the choroid plexus epithelium, causing brain tumors with p53-induced apoptosis (Yin et al. 1997). Using this TgT_{121} model of brain tumors, *E2F1* deficiency caused a significant reduction in the growth of choroid plexus tumors through reduced proliferative expansion of the tumor cells that was counterbalanced by an 80% reduction in p53-dependent apoptosis (Pan et al. 1998). The Alb–Cre *Foxm1b*$^{-/-}$ hepatocytes differ from the *E2F1*$^{-/-}$ brain tumors in that *Foxm1b* deficiency causes a more complete block in proliferative expansion during liver tumor growth without influencing apoptosis. *Foxm1b* deficiency completely prevented development of liver tumors after 33 wk of DEN/PB exposure, a treatment sufficient to cause HCC tumors in control male mice.

Expression of genetically altered forms of several other Fox transcription factors has been implicated in tumorigenesis, including the mammalian FKHR (FoxO1) and the avian Qin (Foxg1) genes (Li and Vogt 1993; Barr et al. 1996). The Avian Sarcoma virus 31 expresses the Qin oncoprotein, a GAG–Foxg1 transcriptional repressor fusion protein that causes transformation of avian embryo fibroblasts in vitro and fibrosarcomas in chickens (Li and Vogt 1993; Chang et al. 1996; Li et al. 1997). Chromosome translocations between either Pax3 or Pax7 and FoxO1 (FKHR) transcription factors create a fusion protein that is a more potent Pax3/7 transcriptional activator, which stimulates target genes involved in cellular transformation (Barr et al. 1996; Scheidler et al. 1996; Barr 2001). Furthermore, activation of Akt kinase is essential for progression into S phase, because AKT inhibits FoxO4 (AFX)/FoxO3a (FKHR-L1)-mediated transcription of the Cdk inhibitor $p27^{Kip1}$ (Medema et al. 2000) and the retinoblastoma-like p130 genes (Kops et al. 2002) and inhibits FoxO1 transcription of pro-apoptotic target genes (Brunet et al. 1999). Unlike the FoxO proteins, whose transcriptional inhibition is required for cell cycle progression, expression of Foxm1b is essential for the proliferative expansion of tumor cells through dimin-

ished nuclear accumulation of $p27^{Kip1}$ protein and stimulation of Cdk-1 activator Cdc25B.

In summary, we demonstrate that *Foxm1b*$^{-/-}$ mouse livers fail to proliferate and are highly resistant to developing HCC after DEN/PB exposure. This resistance of *Foxm1b*$^{-/-}$ hepatocytes to developing liver tumors was associated with aberrant increase in hepatocyte nuclear levels of Cdk inhibitor $p27^{Kip1}$ protein and diminished expression of the M-phase-promoting Cdc25B phosphatase. Furthermore, we showed that DEN/PB exposure caused a transient increase in hepatic expression of the $p19^{ARF}$ tumor suppressor, and that Foxm1b is a novel target for $p19^{ARF}$-mediated transcriptional inhibition. We propose that the transient induction of p19 protein levels may inhibit Foxm1b activity, thereby preventing hepatocyte proliferation early in the process of DEN/PB tumor promotion (Fig. 9J). Furthermore, a membrane transducing $(D\text{-}Arg)_9$ $p19^{ARF}$ 26–44 peptide was found to significantly diminish Foxm1b stimulation of colony formation of U2OS cells on soft agar, suggesting that this $p19^{ARF}$ peptide is an effective therapeutic inhibitor of Foxm1b transformation function. These studies demonstrate that the Foxm1b transcription factor is required for proliferative expansion during tumor progression and constitutes a new potential target for human HCC tumor therapy to diminish proliferation of this aggressive liver cancer.

Materials and methods

DEN/PB liver tumor induction protocol

Generation of the mice containing the *Foxm1b* LoxP/LoxP (fl/fl) targeted allele, which were bred into the C57BL/6 background for four generations, was described previously (Wang et al. 2002a). Conditional deletion of the *Foxm1b* fl/fl allele in adult hepatocytes was accomplished through breeding with the Alb–Cre C57BL/6 transgenic mice (Postic and Magnuson 2000), which were purchased from Jackson Labs. To determine whether *Foxm1b*$^{-/-}$ hepatocytes are refractory to formation of hepatocellular adenomas and carcinomas, we subjected Alb–Cre *Foxm1b*$^{-/-}$ and *Foxm1b* fl/fl (control) mice to a DEN/PB liver tumor-induction protocol (Tamano et al. 1994; Sargent et al. 1996; Kalinina et al. 2003). *Foxm1b* fl/fl male mice were mated with female Alb–Cre *Foxm1b* fl/fl C57BL/6 mice to generate *Foxm1b* fl/fl (control) and Alb–Cre *Foxm1b*$^{-/-}$ (experimental) offspring. At 14 d postnatally, the entire mouse litter received single IP injections of the tumor initiator DEN (5 µg of DEN/g body weight; Sigma, catalog no. N0756), which induces hepatocyte DNA damage through DNA adduct formation. Two weeks following injection of the tumor initiator DEN, the mice were administered the liver tumor promoter PB by providing them water containing 0.05% of PB for the duration of the liver tumor-induction experiment (Tamano et al. 1994; Sargent et al. 1996; Kalinina et al. 2003). We sacrificed *Foxm1b* fl/fl mice and Alb–Cre *Foxm1b*$^{-/-}$ mice at 6, 23, 33, or 50 wk after DEN injection to examine dissected livers for tumors. The liver tissue was used to prepare total protein extracts for Western blot analysis (Rausa et al. 2000) or used for paraffin embedding to prepare 5-µm liver sections (Wang et al. 2002a).

BrdU labeling, immunohistochemical staining, and TUNEL apoptosis assay

To monitor hepatic cellular proliferation, PB was removed 4 d prior to the completion of the experiment, and mice were placed on drinking water with 1 mg/mL of 5-bromo-2′-deoxyuridine (BrdU) for 4 d before they were sacrificed (Ledda-Columbano et al. 2002). Liver sections were histologically stained with H&E and hepatocyte DNA replication was determined by immunofluorescent detection of BrdU incorporation. Rabbit polyclonal antibodies specific to Foxm1b (Ye et al. 1997, 1999), $p27^{kip1}$ (Cell Signaling), $p21^{Cip1}$ and CAR (both from Santa Cruz Biotech), AFP and GST-pi (both from Dako Corp.) proteins were used for immunohistochemical detection of 5-µm liver sections using methods described previously (Ye et al. 1997, 1999; Wang et al. 2002b). To measure apoptosis in mouse livers isolated from either untreated or DEN/PB-treated *Foxm1b* fl/fl and Alb–Cre *Foxm1b*$^{-/-}$ mice (6, 23, or 33 weeks), TUNEL assay was performed on liver sections using the ApoTag Red in situ apoptosis detection kit from Intergen according to the manufacturer's recommendations. Centromere-specific mouse FISH probe was purchased from Vysis Inc. and used to hybridize paraffin-embedded liver sections according to manufacture's protocol. We calculated the mean number (±S.D.) of $p27^{Kip1}$, BrdU, TUNEL, or DAPI-positive hepatocyte nuclei per 1000 cells or 200× field by counting the number of positive hepatocyte nuclei using five different 200× liver sections from three distinct male mice at the indicated times of DEN/PB exposure or untreated.

Western blot analysis, Co-IP assays

For Western blot analysis, 100 µg of total protein extracts prepared from liver (Rausa et al. 2000) were separated on SDS-PAGE and transferred to PVDF membrane (Bio-Rad). For Western blot analysis, we used rabbit antibodies specific to either $p27^{Kip1}$ (Cell Signaling; 1:1000), $p19^{ARF}$ (AB80; GeneTex; 1:750) Cdk2, Cdc25B, or Cdc25C (all from Santa Cruz Biotech, 1:1000) proteins. The primary antibody signals were amplified by HRP-conjugated secondary antibodies (Bio-Rad) and detected with Enhanced Chemiluminescence Plus (ECL-plus, Amersham Pharmacia Biotech). Western blot analysis was performed with liver extracts from two mice per indicated time points following DEN/PB treatment and signal intensities were normalized to Cdk2 signals. Quantitation of expression levels was determined with Tiff files from scanned films by using the BioMax 1D program (Kodak).

To define the $p19^{ARF}$ sequences that are sufficient to associate with and inhibit Foxm1b transcriptional activity, we used PCR amplification with primers to introduce the protein transduction/nuclear localization domain (MGYGRKKRRQRRR) from the HIV-TAT protein (Becker-Hapak et al. 2001) at the N terminus of either the $p19^{ARF}$ sequences 26–44 or 26–55. For both constructs, we used the sense HindIII ATG-TAT mouse p19 (26–34) primer CTCAAGCTTAACATGGGCTACGGCCGC AAGAAACGCCGCCAGCGCCGCCGCAAGTTCGTGCGAT CCCGGAGACCC, the antisense EcoR1 p19 45–37 primer CT CGAATTCGTTCACGAAAGCCAGAGCGCAGCT, and the antisense EcoR1 p19 55–48 primer CTCGAATTCTCTTCT CAAGATCCTCTCTAGCCT (underlined is the HindIII or EcoR1 restriction enzyme sequence). The PCR products were digested with HindIII and EcoR1 and the TAT-p19 sequences were cloned in-frame with the V5 epitope/polyhistidine tag in the corresponding sites in the CMV promoter containing pcDNA3.1/V5-His A expression vector (Invitrogen). We also cloned the HindIII and EcoR1 TAT-p19 sequences into the corresponding sites of the CMV pEGFP expression vector (Clontech).

U2OS cells were plated on 100-mm plates and transiently transfected with 5 µg of CMV GFP–Foxm1b or CMV HA-epitope-tagged wild-type $p19^{ARF}$ or CMV expression plasmids containing HA tagged N-terminal deletion mutants of the $p19^{ARF}$ protein (Δ1–14, Δ15–25, Δ26–37, or Δ26–37 + Δ1–14) or V5-TAT-$p19^{ARF}$ proteins (26–44 or 26–55). Transfected cells were harvested at 48 h following transfection in PBS, pelleted by centrifugation, and used to make total cell protein extracts using the NP40 lysis buffer as described previously (Major et al. 2004). The NP40 lysis buffer consisted of 50 mM Tris (pH 7.5), 100 mM NaCl, 5 mM EDTA, 5 mM EGTA, 1% NP40, 5% Glycerol, and freshly added 1× Complete Mini protease inhibitor cocktail (Roche), 2 mM PMSF and phosphatase inhibitors, 20-mM β-glycerolphosphate, 2 mM NaF, and 2 mM $NaVO_4$. The HA epitope tag antibody (Roche; 2 µg/Co-IP) was used to immunoprecipitate the $p19^{ARF}$ protein from U2OS lysates (500 µg) transfected with CMV GFP–Foxm1b and CMV expression vectors containing either wild-type HA-$p19^{ARF}$ or N-terminal mutant HA-$p19^{ARF}$ proteins, and then subjected to Western blot analysis with a monoclonal antibody against the GFP protein (Clontech). We also used the V5 epitope tag antibody (Invitrogen; 2 µg/Co-IP) to immunoprecipitate the $p19^{ARF}$ protein from U2OS lysates (500 µg) transfected with CMV GFP–Foxm1b and CMV expression vector containing either V5-TAT-$p19^{ARF}$ 26–44 or V5-TAT-$p19^{ARF}$ 26–55, and then subjected to Western blot analysis with a monoclonal antibody against the GFP protein (Clontech).

For Co-IP experiments, 500 µg of protein extract prepared from either untransfected passage 12 MEFs or DEN/PB-treated liver was immunoprecipitated with $p19^{ARF}$ antibody (AB80; GeneTex; 2 µg), followed by Western Blot analysis with mouse antibody Foxm1b protein (1:5000). The signals from the primary antibody were amplified by HRP-conjugated anti-mouse IgG (Bio-Rad), and detected with Enhanced Chemiluminescence Plus (ECL-plus, Amersham Pharmacia Biotech).

Foxm1b and p19 cotransfection assays and synthesis of (D-Arg)$_9$-p19^{ARF}26–44 peptide

Human osteosarcoma U2OS cells were maintained in DMEM supplemented with 10% fetal calf serum, 1× Pen/Strep, and 1× L-Glutamine (GIBCO). For transient transfection, U2OS cells were plated in six-well plates and transfected using Fugene 6 reagent (Roche) according to the manufacturer's protocol. Cells were transfected with 500 ng of CMV wild-type Foxm1b 1–748 alone or with CMV expression vectors containing either wild-type T7-$p19^{ARF}$ or N-terminal mutant T7-$p19^{ARF}$ protein (Δ1–14, Δ15–25, Δ26–37, or Δ26–37 + Δ1–14) or V5-TAT-$p19^{ARF}$ 26–44 or V5-TAT-$p19^{ARF}$ 26–55 sequences and with 1.5 µg of a 6× Foxm1b TATA-Luciferase reporter. We also included 10 ng of CMV-Renilla luciferase reporter plasmid as an internal control to normalize transfection efficiency. Cotransfection assays were also performed with 500 ng of CMV Foxm1b 1–688 and 6× Foxm1b TATA-Luciferase reporter and 10 ng of CMV-Renilla internal control. Twenty-four hours posttransfection, cells were prepared for dual luciferase assays (Promega). Luciferase activity was determined as percent of wild-type Foxm1b activity following normalization to Renilla activity. Experiments were performed at least four times in triplicate and mean ± S.D. determined.

The Sigma-Genosys company (The Woodlands) synthesized a (D-Arg)$_9$-p19ARF 26–44 peptide (rrrrrrrrrKFVRSRRPRTASCALAFVN) containing nine D-Arg residues at the N terminus, which has been demonstrated to enhance cellular uptake of polypeptides (Wender et al. 2000). The (D-Arg)$_9$-p19ARF 26–44 peptide is tagged with a fluorescent Lissamine (TRITC) on the N terminus and acetylated at the C terminus and was purified by high-pressure liquid chromatography (Sigma-Genosys). Cotransfection assays were also performed with 500 ng of CMV Foxm1b 1–688, 6× Foxm1b TATA-Luciferase reporter, and 10 ng of CMV-Renilla internal control. The transfected U2OS cells were treated with 12 µM of the $p19^{ARF}$ rrrrrrrrrKFVRSRRPRTASCALAFVN peptide for 24 h, and then harvested for dual luciferase assays (Promega) as described above.

U2OS cells were transiently transfected in two-well chamber slides (Nunc) with CMV GFP–Foxm1b expression constructs in the presence or absence of either CMV wild-type T7-$p19^{ARF}$, CMV HA-$p19^{ARF}$, or CMV expression constructs containing either N-terminal mutant T7-$p19^{ARF}$ proteins (Δ1–14, Δ15–25, or Δ26–37) or V5-TAT-$p19^{ARF}$ proteins (26–44 or 26–55). We also transiently transfected U2OS cells with CMV EGFP expression vector containing the TAT-$p19^{ARF}$ proteins (26–44 or 26–55). Forty-eight hours posttransfection, cells were fixed in 4% paraformaldehyde for 20 min at room temperature. GFP fluorescence or immunofluorescence with anti-HA antibody following TRITC-conjugated secondary antibody was detected using a Zeiss microscope. U2OS cells were treated with 12 µM of the rrrrrrrrrKFVRSRRPRTASCALAFVN peptide for 24 h, and then analyzed for TRITC fluorescence as described above.

Creation of doxycycline-inducible CMV-TETO GFP–Foxm1b U2OS cell line and soft agar assays

The T-REx-U2OS cells were purchased from Invitrogen Life Technologies (catalog no. R712-07). The T-REx-U2OS cells express the Tet repressor from pCEP4/*tet*R that is episomally maintained in tissue culture medium containing 10% fetal calf serum and drug selection with 50 µg/mL of Hygromycin B. Tetracycline regulation in the T-REx System is based on the binding of tetracycline to the TET repressor and derepressing of the CMV-TETO promoter controlling expression of the gene of interest (Yao et al. 1998). We generated the pCDNA4-TO GFP–Foxm1b expression plasmid provided in the T-REx system as described previously (Major et al. 2004) and transfected T-REx-U2OS cells with linearized pCDNA4-TO GFP–Foxm1b expression plasmid to select clonal doxycycline inducible GFP–Foxm1b U2OS cell lines. CMV-TETO GFP–Foxm1b U2OS clones were isolated by selection for 3 wk with tissue culture medium containing 50 µg/mL of Hygromycin B and 250 µg/mL of Zeocin. The CMV-TETO GFP–Foxm1b U2OS clone C3 cell line was selected for the soft agar assays because it exhibited intermediate expression of the GFP–Foxm1b fusion protein in response to 1 µg/mL of Doxycycline (Sigma D-9891) as determined by Western blot analysis with GFP monoclonal antibody. Wild-type U2OS cells or CMV-TETO GFP–Foxm1b U2OS clone C3 cells were grown in medium with or without 1 µg/mL of Doxycycline for 2 d prior to either adding the (D-Arg)$_9$-$p19^{ARF}$ 26–44 peptide or left untreated. We then added 12 µM of this $p19^{ARF}$ peptide (rrrrrrrrrKFVRSRRPRTASCALAFVN) for 24 h prior to splitting the cells for the soft agar assays using procedures described previously (Conzen et al. 2000). U2OS cells (10^5) were plated subconfluently in a six-well plates in 0.7% agarose on a 1.4% agarose bed in the presence or absence of 12 µM of the (D-Arg)$_9$-$p19^{ARF}$ 26–44 peptide and 1 µg/mL of Doxycycline. Every 4 d, the tissue-culture medium containing 10% fetal calf serum, 12 µM of the (D-Arg)$_9$-$p19^{ARF}$ 26–44 peptide, and 1 µg/mL of doxycycline was replaced. Controls included growth in medium containing 10% fetal calf serum with or without 1 µg/mL of Doxycycline. U2OS cell colonies that were larger than 1 mm in size were scored after 2 wk of growth on the soft agar.

Acknowledgments

We thank H. Kiyokawa (UIC), I.-C. Wang (UIC), and A. Columbano (University of Cagliari, Italy) for critically reviewing the manuscript. We also thank S.E. Crawford (Northwestern University Medical School) for help with identification of the type of liver tumors, H. Kiyokawa (UIC) for providing us with the CMV $p27^{Kip1}$ expression vector, and Nissim Hay's laboratory (UIC) for help with the soft agar assays. This work was supported by US Public Health Service Grants DK 54687-06 from NIDDK (R.H.C.) and RO1 AG 21842-02 from NIA (R.H.C.).

The publication costs of this article were defrayed in part by payment of page charges. This article must therefore be hereby marked "advertisement" in accordance with 18 USC section 1734 solely to indicate this fact.

References

Alkarain, A. and Slingerland, J. 2004. Deregulation of p27 by oncogenic signaling and its prognostic significance in breast cancer. *Breast Cancer Res.* **6:** 13–21.

Barr, F.G. 2001. Gene fusions involving PAX and FOX family members in alveolar rhabdomyosarcoma. *Oncogene* **20:** 5736–5746.

Barr, F.G., Nauta, L.E., Davis, R.J., Schafer, B.W., Nycum, L.M., and Biegel, J.A. 1996. In vivo amplification of the PAX3–FKHR and PAX7–FKHR fusion genes in alveolar rhabdomyosarcoma. *Hum. Mol. Genet.* **5:** 15–21.

Becker-Hapak, M., McAllister, S.S., and Dowdy, S.F. 2001. TAT-mediated protein transduction into mammalian cells. *Methods* **24:** 247–256.

Block, T.M., Mehta, A.S., Fimmel, C.J., and Jordan, R. 2003. Molecular viral oncology of hepatocellular carcinoma. *Oncogene* **22:** 5093–5107.

Brunet, A., Bonni, A., Zigmond, M.J., Lin, M.Z., Juo, P., Hu, L.S., Anderson, M.J., Arden, K.C., Blenis, J., and Greenberg, M.E. 1999. Akt promotes cell survival by phosphorylating and inhibiting a Forkhead transcription factor. *Cell* **96:** 857–868.

Chang, H.W., Li, J., and Vogt, P.K. 1996. Domains of the qin protein required for oncogenic transformation. *Oncogene* **13:** 441–444.

Chawla, A., Repa, J.J., Evans, R.M., and Mangelsdorf, D.J. 2001. Nuclear receptors and lipid physiology: Opening the X-files. *Science* **294:** 1866–1870.

Chen, H., Egan, J.O., and Chiu, J.F. 1997. Regulation and activities of a-fetoprotein. *Crit. Rev. Eukaryot. Gene Expr.* **7:** 11–41.

Clark, K.L., Halay, E.D., Lai, E., and Burley, S.K. 1993. Co-crystal structure of the HNF-3/fork head DNA-recognition motif resembles histone H5. *Nature* **364:** 412–420.

Conzen, S.D., Gottlob, K., Kandel, E.S., Khanduri, P., Wagner, A.J., O'Leary, M., and Hay, N. 2000. Induction of cell cycle progression and acceleration of apoptosis are two separable functions of c-Myc: Transrepression correlates with acceleration of apoptosis. *Mol. Cell. Biol.* **20:** 6008–6018.

Costa, R.H., Kalinichenko, V.V., Holterman, A.X., and Wang, X. 2003. Transcription factors in liver development, differentiation, and regeneration. *Hepatology* **38:** 1331–1347.

Datta, A., Nag, A., and Raychaudhuri, P. 2002. Differential regulation of E2F1, DP1, and the E2F1/DP1 complex by ARF. *Mol. Cell. Biol.* **22:** 8398–8408.

Eferl, R., Ricci, R., Kenner, L., Zenz, R., David, J.P., Rath, M., and Wagner, E.F. 2003. Liver tumor development. c-Jun antagonizes the proapoptotic activity of p53. *Cell* **112:** 181–192.

Factor, V., Oliver, A.L., Panta, G.R., Thorgeirsson, S.S., Sonenshein, G.E., and Arsura, M. 2001. Roles of Akt/PKB and IKK complex in constitutive induction of NF-κB in hepatocellular carcinomas of transforming growth factor α/c-myc transgenic mice. *Hepatology* **34:** 32–41.

Gomez-Angelats, M., Teeguarden, J.G., Dragan, Y.P., and Pitot, H.C. 1999. Mutational analysis of three tumor suppressor genes in two models of rat hepatocarcinogenesis. *Mol. Carcinog.* **25:** 157–163.

Graveel, C.R., Jatkoe, T., Madore, S.J., Holt, A.L., and Farnham, P.J. 2001. Expression profiling and identification of novel genes in hepatocellular carcinomas. *Oncogene* **20:** 2704–2712.

Harbour, J.W. and Dean, D.C. 2000. The Rb/E2F pathway: Expanding roles and emerging paradigms. *Genes & Dev.* **14:** 2393–2409.

Hatayama, I., Nishimura, S., Narita, T., and Sato, K. 1993. Sex-dependent expression of class pi glutathione S-transferase during chemical hepatocarcinogenesis in B6C3F1 mice. *Carcinogenesis* **14:** 537–538.

Ishida, S., Huang, E., Zuzan, H., Spang, R., Leone, G., West, M., and Nevins, J.R. 2001. Role for E2F in control of both DNA replication and mitotic functions as revealed from DNA microarray analysis. *Mol. Cell. Biol.* **21:** 4684–4699.

Kaestner, K.H., Knochel, W., and Martinez, D.E. 2000. Unified nomenclature for the winged helix/forkhead transcription factors. *Genes & Dev.* **14:** 142–146.

Kalinichenko, V.V., Gusarova, G.A., Tan, Y., Wang, I.C., Major, M.L., Wang, X., Yoder, H.M., and Costa, R.H. 2003. Ubiquitous expression of the forkhead box M1B transgene accelerates proliferation of distinct pulmonary cell-types following lung injury. *J. Biol. Chem.* **278:** 37888–37894.

Kalinina, O.A., Kalinin, S.A., Polack, E.W., Mikaelian, I., Panda, S., Costa, R.H., and Adami, G.R. 2003. Sustained hepatic expression of FoxM1B in transgenic mice has minimal effects on hepatocellular carcinoma development but increases cell proliferation rates in preneoplastic and early neoplastic lesions. *Oncogene* **22:** 6266–6276.

Kamijo, T., Zindy, F., Roussel, M.F., Quelle, D.E., Downing, J.R., Ashmun, R.A., Grosveld, G., and Sherr, C.J. 1997. Tumor suppression at the mouse INK4a locus mediated by the alternative reading frame product p19ARF. *Cell* **91:** 649–659.

Kamijo, T., Bodner, S., van de Kamp, E., Randle, D.H., and Sherr, C.J. 1999. Tumor spectrum in ARF-deficient mice. *Cancer Res.* **59:** 2217–2222.

Kops, G.J., Medema, R.H., Glassford, J., Essers, M.A., Dijkers, P.F., Coffer, P.J., Lam, E.W., and Burgering, B.M. 2002. Control of cell cycle exit and entry by protein kinase B-regulated forkhead transcription factors. *Mol. Cell. Biol.* **22:** 2025–2036.

Korver, W., Roose, J., and Clevers, H. 1997. The winged-helix transcription factor Trident is expressed in cycling cells. *Nucleic Acids Res.* **25:** 1715–1719.

Korver, W., Schilham, M.W., Moerer, P., van den Hoff, M.J., Dam, K., Lamers, W.H., Medema, R.H., and Clevers, H. 1998. Uncoupling of S phase and mitosis in cardiomyocytes and hepatocytes lacking the winged-helix transcription factor trident. *Curr. Biol.* **8:** 1327–1330.

Krupczak-Hollis, K., Wang, X., Dennewitz, M.B., and Costa, R.H. 2003. Growth hormone stimulates proliferation of old-aged regenerating liver through forkhead box m1b. *Hepatology* **38:** 1552–1562.

Kunnath, L. and Locker, J. 1983. Developmental changes in the methylation of the rat albumin and α-fetoprotein genes. *EMBO J.* **2:** 317–324.

Kwon, Y.H., Jovanovic, A., Serfas, M.S., Kiyokawa, H., and

Tyner, A.L. 2002. P21 functions to maintain quiescence of p27-deficient hepatocytes. *J. Biol. Chem.* **277:** 41417–41422.
Ledda-Columbano, G.M., Pibiri, M., Concas, D., Cossu, C., Tripodi, M., and Columbano, A. 2002. Loss of cyclin D1 does not inhibit the proliferative response of mouse liver to mitogenic stimuli. *Hepatology* **36:** 1098–1105.
Li, J. and Vogt, P.K. 1993. The retroviral oncogene qin belongs to the transcription factor family that includes the homeotic gene fork head. *Proc. Natl. Acad. Sci.* **90:** 4490–4494.
Li, J., Thurm, H., Chang, H.W., Iacovoni, J.S., and Vogt, P.K. 1997. Oncogenic transformation induced by the qin protein is correlated with transcriptional repression. *Proc. Natl. Acad. Sci.* **94:** 10885–10888.
Liang, J., Zubovitz, J., Petrocelli, T., Kotchetkov, R., Connor, M.K., Han, K., Lee, J.H., Ciarallo, S., Catzavelos, C., Beniston, R., et al. 2002. PKB/Akt phosphorylates p27, impairs nuclear import of p27 and opposes p27-mediated G1 arrest. *Nat. Med.* **8:** 1153–1160.
Major, M.L., Lepe, R., and Costa, R.H. 2004. Forkhead box M1B (FoxM1B) transcriptional activity requires binding of Cdk/Cyclin complexes for phosphorylation-dependent recruitment of p300/CBP co-activators. *Mol. Cell. Biol.* **24:** 2649–2661.
Martelli, F., Hamilton, T., Silver, D.P., Sharpless, N.E., Bardeesy, N., Rokas, M., DePinho, R.A., Livingston, D.M., and Grossman, S.R. 2001. p19ARF targets certain E2F species for degradation. *Proc. Natl. Acad. Sci.* **98:** 4455–4460.
Medema, R.H., Kops, G.J., Bos, J.L., and Burgering, B.M. 2000. AFX-like Forkhead transcription factors mediate cell-cycle regulation by Ras and PKB through p27kip1. *Nature* **404:** 782–787.
Nilsson, I. and Hoffmann, I. 2000. Cell cycle regulation by the Cdc25 phosphatase family. *Prog. Cell Cycle Res.* **4:** 107–114.
Okabe, H., Satoh, S., Kato, T., Kitahara, O., Yanagawa, R., Yamaoka, Y., Tsunoda, T., Furukawa, Y., and Nakamura, Y. 2001. Genome-wide analysis of gene expression in human hepatocellular carcinomas using cDNA microarray: Identification of genes involved in viral carcinogenesis and tumor progression. *Cancer Res.* **61:** 2129–2137.
Palmero, I., Pantoja, C., and Serrano, M. 1998. p19ARF links the tumour suppressor p53 to Ras. *Nature* **395:** 125–126.
Pan, H., Yin, C., Dyson, N.J., Harlow, E., Yamasaki, L., and Van Dyke, T. 1998. Key roles for E2F1 in signaling p53-dependent apoptosis and in cell division within developing tumors. *Mol. Cell* **2:** 283–292.
Polyak, K., Kato, J.Y., Solomon, M.J., Sherr, C.J., Massague, J., Roberts, J.M., and Koff, A. 1994. p27Kip1, a cyclin-Cdk inhibitor, links transforming growth factor-β and contact inhibition to cell cycle arrest. *Genes & Dev.* **8:** 9–22.
Pomerantz, J., Schreiber-Agus, N., Liegeois, N.J., Silverman, A., Alland, L., Chin, L., Potes, J., Chen, K., Orlow, I., Lee, H.W., et al. 1998. The Ink4a tumor suppressor gene product, p19Arf, interacts with MDM2 and neutralizes MDM2's inhibition of p53. *Cell* **92:** 713–723.
Porter, P.L., Malone, K.E., Heagerty, P.J., Alexander, G.M., Gatti, L.A., Firpo, E.J., Daling, J.R., and Roberts, J.M. 1997. Expression of cell-cycle regulators p27Kip1 and cyclin E, alone and in combination, correlate with survival in young breast cancer patients. *Nat. Med.* **3:** 222–225.
Postic, C. and Magnuson, M.A. 2000. DNA excision in liver by an albumin–Cre transgene occurs progressively with age. *Genesis* **26:** 149–150.
Quelle, D.E., Zindy, F., Ashmun, R.A., and Sherr, C.J. 1995. Alternative reading frames of the INK4a tumor suppressor gene encode two unrelated proteins capable of inducing cell cycle arrest. *Cell* **83:** 993–1000.
Rausa, F.M., Tan, Y., Zhou, H., Yoo, K., Stolz, D.B., Watkins, S., Franks, R.R., Unterman, T.G., and Costa, R.H. 2000. Elevated levels of HNF-3b in mouse hepatocytes influence expression of genes involved in bile acid and glucose homeostasis. *Mol. Cell. Biol.* **20:** 8264–8282.
Rausa, F., Tan, Y., and Costa, R.H. 2003. Association between HNF-6 and FoxA2 DNA binding domains stimulates FoxA2 transcriptional activity but inhibits HNF-6 DNA binding. *Mol. Cell. Biol.* **23:** 437–449.
Sanders, S. and Thorgeirsson, S.S. 1999. Phenobarbital promotes liver growth in c-myc/TGF-α transgenic mice by inducing hypertrophy and inhibiting apoptosis. *Carcinogenesis* **20:** 41–49.
Sandgren, E.P., Quaife, C.J., Pinkert, C.A., Palmiter, R.D., and Brinster, R.L. 1989. Oncogene-induced liver neoplasia in transgenic mice. *Oncogene* **4:** 715–724.
Sandgren, E.P., Luetteke, N.C., Qiu, T.H., Palmiter, R.D., Brinster, R.L., and Lee, D.C. 1993. Transforming growth factor a dramatically enhances oncogene-induced carcinogenesis in transgenic mouse pancreas and liver. *Mol. Cell. Biol.* **13:** 320–330.
Sargent, L., Dragan, Y., Xu, Y.H., Sattler, G., Wiley, J., and Pitot, H.C. 1996. Karyotypic changes in a multistage model of chemical hepatocarcinogenesis in the rat. *Cancer Res.* **56:** 2985–2991.
Scheidler, S., Fredericks, W.J., Rauscher III, F.J., Barr, F.G., and Vogt, P.K. 1996. The hybrid PAX3–FKHR fusion protein of alveolar rhabdomyosarcoma transforms fibroblasts in culture. *Proc. Natl. Acad. Sci.* **93:** 9805–9809.
Sebastian, B., Kakizuka, A., and Hunter, T. 1993. Cdc25M2 activation of cyclin-dependent kinases by dephosphorylation of threonine-14 and tyrosine-15. *Proc. Natl. Acad. Sci.* **90:** 3521–3524.
Sherr, C.J. 1998. Tumor surveillance via the ARF-p53 pathway. *Genes & Dev.* **12:** 2984–2991.
Sherr, C.J. and McCormick, F. 2002. The RB and p53 pathways in cancer. *Cancer Cell* **2:** 103–112.
Sherr, C.J. and Roberts, J.M. 1999. CDK inhibitors: Positive and negative regulators of G1-phase progression. *Genes & Dev.* **13:** 1501–1512.
Shin, I., Yakes, F.M., Rojo, F., Shin, N.Y., Bakin, A.V., Baselga, J., and Arteaga, C.L. 2002. PKB/Akt mediates cell-cycle progression by phosphorylation of $p27^{Kip1}$ at threonine 157 and modulation of its cellular localization. *Nat. Med.* **8:** 1145–1152.
Steele, P.R., Yim, A.P., Herbertson, B.M., and Watson, J. 1981. Some flow cytofluorimetric studies of the nuclear ploidy of mouse hepatocytes. II. Early changes in nuclear ploidy of mouse hepatocytes following carbon tetrachloride administration: Evidence for polyploid nuclei arrested in telophase. *Br. J. Exp. Pathol.* **62:** 474–479.
Tamano, S., Merlino, G.T., and Ward, J.M. 1994. Rapid development of hepatic tumors in transforming growth factor a transgenic mice associated with increased cell proliferation in precancerous hepatocellular lesions initiated by N-nitrosodiethylamine and promoted by phenobarbital. *Carcinogenesis* **15:** 1791–1798.
Teh, M.T., Wong, S.T., Neill, G.W., Ghali, L.R., Philpott, M.P., and Quinn, A.G. 2002. FOXM1 is a downstream target of Gli1 in basal cell carcinomas. *Cancer Res.* **62:** 4773–4780.
Thorgeirsson, S.S., Teramoto, T., and Factor, V.M. 1998. Dysregulation of apoptosis in hepatocellular carcinoma. *Semin. Liver Dis.* **18:** 115–122.
Trembley, J.H., Ebbert, J.O., Kren, B.T., and Steer, C.J. 1996. Differential regulation of cyclin B1 RNA and protein expression during hepatocyte growth in vivo. *Cell Growth Differ.* **7:** 903–916.

van den Boom, J., Wolter, M., Kuick, R., Misek, D.E., Youkilis, A.S., Wechsler, D.S., Sommer, C., Reifenberger, G., and Hanash, S.M. 2003. Characterization of gene expression profiles associated with glioma progression using oligonucleotide-based microarray analysis and real-time reverse transcription-polymerase chain reaction. *Am. J. Pathol.* **163:** 1033–1043.

Varela, M., Sala, M., Llovet, J.M., and Bruix, J. 2003. Treatment of hepatocellular carcinoma: Is there an optimal strategy? *Cancer Treat Rev.* **29:** 99–104.

Viglietto, G., Motti, M.L., Bruni, P., Melillo, R.M., D'Alessio, A., Califano, D., Vinci, F., Chiappetta, G., Tsichlis, P., Bellacosa, A., et al. 2002. Cytoplasmic relocalization and inhibition of the cyclin-dependent kinase inhibitor p27(Kip1) by PKB/Akt-mediated phosphorylation in breast cancer. *Nat. Med.* **8:** 1136–1144.

Wang, X., Hung, N.-J., and Costa, R.H. 2001a. Earlier expression of the transcription factor HFH 11B (FOXM1B) diminishes induction of $p21^{CIP1/WAF1}$ levels and accelerates mouse hepatocyte entry into S-phase following carbon tetrachloride liver injury. *Hepatology* **33:** 1404–1414.

Wang, X., Quail, E., Hung, N.-J., Tan, Y., Ye, H., and Costa, R.H. 2001b. Increased levels of Forkhead Box M1B transcription factor in transgenic mouse hepatocytes prevents age-related proliferation defects in regenerating liver. *Proc. Natl. Acad. Sci.* **98:** 11468–11473.

Wang, X., Kiyokawa, H., Dennewitz, M.B., and Costa, R.H. 2002a. The Forkhead Box m1b transcription factor is essential for hepatocyte DNA replication and mitosis during mouse liver regeneration. *Proc. Natl. Acad. Sci.* **99:** 16881–16886.

Wang, X., Krupczak-Hollis, K., Tan, Y., Dennewitz, M.B., Adami, G.R., and Costa, R.H. 2002b. Increased hepatic Forkhead Box M1B (FoxM1B) levels in old-aged mice stimulated liver regeneration through diminished p27Kip1 protein levels and increased Cdc25B expression. *J. Biol. Chem.* **277:** 44310–44316.

Weber, J.D., Taylor, L.J., Roussel, M.F., Sherr, C.J., and Bar-Sagi, D. 1999. Nucleolar Arf sequesters Mdm2 and activates p53. *Nat. Cell. Biol.* **1:** 20–26.

Weber, J.D., Kuo, M.L., Bothner, B., DiGiammarino, E.L., Kriwacki, R.W., Roussel, M.F., and Sherr, C.J. 2000. Cooperative signals governing ARF–mdm2 interaction and nucleolar localization of the complex. *Mol. Cell. Biol.* **20:** 2517–2528.

Weihrauch, M., Benick, M., Lehner, G., Wittekind, M., Bader, M., Wrbitzk, R., and Tannapfel, A. 2001. High prevalence of K-ras-2 mutations in hepatocellular carcinomas in workers exposed to vinyl chloride. *Int. Arch. Occup. Environ. Health* **74:** 405–410.

Wender, P.A., Mitchell, D.J., Pattabiraman, K., Pelkey, E.T., Steinman, L., and Rothbard, J.B. 2000. The design, synthesis, and evaluation of molecules that enable or enhance cellular uptake: Peptoid molecular transporters. *Proc. Natl. Acad. Sci.* **97:** 13003–13008.

Wu, J.C., Merlino, G., Cveklova, K., Mosinger Jr., B., and Fausto, N. 1994. Autonomous growth in serum-free medium and production of hepatocellular carcinomas by differentiated hepatocyte lines that overexpress transforming growth factor a1. *Cancer Res.* **54:** 5964–5973.

Wu, H., Wade, M., Krall, L., Grisham, J., Xiong, Y., and Van Dyke, T. 1996. Targeted in vivo expression of the cyclin-dependent kinase inhibitor p21 halts hepatocyte cell-cycle progression, postnatal liver development and regeneration. *Genes & Dev.* **10:** 245–260.

Yao, K.M., Sha, M., Lu, Z., and Wong, G.G. 1997. Molecular analysis of a novel winged helix protein, WIN. Expression pattern, DNA binding property, and alternative splicing within the DNA binding domain. *J. Biol. Chem.* **272:** 19827–19836.

Yao, F., Svensjo, T., Winkler, T., Lu, M., Eriksson, C., and Eriksson, E. 1998. Tetracycline repressor, tetR, rather than the tetR–mammalian cell transcription factor fusion derivatives, regulates inducible gene expression in mammalian cells. *Hum. Gene Ther.* **9:** 1939–1950.

Ye, H., Kelly, T.F., Samadani, U., Lim, L., Rubio, S., Overdier, D.G., Roebuck, K.A., and Costa, R.H. 1997. Hepatocyte nuclear factor 3/fork head homolog 11 is expressed in proliferating epithelial and mesenchymal cells of embryonic and adult tissues. *Mol. Cell. Biol.* **17:** 1626–1641.

Ye, H., Holterman, A., Yoo, K.W., Franks, R.R., and Costa, R.H. 1999. Premature expression of the winged helix transcription factor HFH-11B in regenerating mouse liver accelerates hepatocyte entry into S-phase. *Mol. Cell. Biol.* **19:** 8570–8580.

Yin, C., Knudson, C.M., Korsmeyer, S.J., and Van Dyke, T. 1997. Bax suppresses tumorigenesis and stimulates apoptosis in vivo. *Nature* **385:** 637–640.

Zerfass-Thome, K., Schulze, A., Zwerschke, W., Vogt, B., Helin, K., Bartek, J., Henglein, B., and Jansen-Durr, P. 1997. p27KIP1 blocks cyclin E-dependent transactivation of cyclin A gene expression. *Mol. Cell. Biol.* **17:** 407–415.

Foxm1b transcription factor is essential for development of hepatocellular carcinomas and is negatively regulated by the p19 ARF tumor suppressor

Vladimir V. Kalinichenko, Michael L. Major, Xinhe Wang, et al.

Genes Dev. 2004, **18:**
Access the most recent version at doi:10.1101/gad.1200704